Hard Copy (HC) $3.00
Microfiche (MF) .65

AMMONIA ADSORPTION AND DECOMPOSITION ON A TUNGSTEN (211) SURFACE*

John W. May,** Roland J. Szostak*** and Lester H. Germer

Department of Applied Physics
Cornell University, Ithaca, New York

ABSTRACT

Interaction of ammonia with a (211) tungsten surface is studied by flash desorption mass spectrometry, low energy electron diffraction, and measurements of work function change. Ammonia adsorbed at room temperature on W(211) is undissociated. Heating to 500°K causes partial decomposition with evolution of hydrogen but not nitrogen, and leaves a residue having stoichiometry NH_2. At about 800°K NH_2 groups are ordered without further decomposition into a centered rectangular array resting upon the substrate. The overlayer and substrate together form a C(4x2) structure. Onset of partial evaporation of the NH_2 layer begins at about 900°K with the rectangular unit mesh of the NH_2 array being continuously stretched in the direction parallel to the troughs of the substrate.

* Research supported by National Aeronautics and Space Administration Contract NGR 33-010-029 and American Iron and Steel Institute Contract No. 148. We gratefully acknowledge the Advanced Research Projects Agency for financial support of this project through the use of the Central Facilities of the Materials Science Center.

** Now at Bartol Research Foundation of the Franklin Institute, Swarthmore, Pennsylvania.

***Present Address -

The maximum stretching amounts to about 12 per cent, with corresponding evolution of nitrogen and hydrogen and stoichiometry apparently remaining NH_2. At 1050°K the rectangular array becomes unstable, and there is a drastic surface rearrangement after which LEED patterns are similar to patterns produced by pure nitrogen, though stoichiometry seems to be still NH_2. Finally, heating to even higher temperatures causes destruction of this "pseudo-nitrogen" NH_2 structure. Nitrogen and atomic H evaporate together in a pressure burst near 1200°K and the surface is completely clean at about 1300°K. NH_3 can be adsorbed as a second weakly held layer on top of an NH_2 primary layer. Kelvin method measurements have shown that the work function is hardly changed by a layer of NH_2, but NH_3 reduces the work function by about one volt whether on bare metal or on top of an NH_2 layer.

INTRODUCTION

Adsorption and decomposition of ammonia on tungsten have been studied for over forty years, but basic understanding has not yet been reached. Polycrystalline surfaces have been used extensively[1-13] and lack of knowledge of surface composition and of surface structure have been severe handicaps. In recent work[14-18] emphasis has been on trying to identify the adsorbed species using well defined surfaces, rather than simply monitoring pressure changes in a flow system at pressures of the order of

1 torr, as in many of the older experiments. In this paper we report an investigation of ammonia adsorption on a tungsten (211) single crystal surface. Conclusions are drawn from flash desorption measurements (I), from LEED determination of surface structures (II), and from work function changes (III).

The behavior of ammonia on a W(211) surface is similar in many ways to its behavior on a W(100) surface recently described by Estrup and Anderson.[18] When these ammonia covered surfaces are heated and the sequence of decomposition products analyzed by mass spectrometer, remarkable parallels are observed although structures on the two surfaces during decomposition are, of course, very different because of the different symmetries. Structural changes are more complex for the (211) surface than for the (100) surface.

EXPERIMENTAL

Three different tungsten crystals were used and all gave identical results. Each was welded to heavy tungsten supports and mounted in a standard Varian Associates LEED system. Temperatures were measured by tungsten-rhenium thermocouples. Gas composition was monitored by a Varian Associates quadrupole mass spectrometer.

When ammonia was admitted large quantities of hydrogen were formed, probably by cracking of ammonia in the sputter-ion pump (Varian Associates, 140 ℓ/sec). Hot filaments of the LEED gun,

mass spectrometer and ion gauge also decomposed ammonia, though decomposition from these sources could be eliminated almost completely by reducing power to the filaments. After this was done the partial pressure of nitrogen was very small, but that of hydrogen still serious. Evidently nitrogen from ammonia-cracking is well gettered by the pump, but hydrogen diffuses back into the system.

Experiments were necessarily conducted in mixtures of ammonia, hydrogen and nitrogen. Relative amounts of these gases depended mainly on the time interval after baking the system. Immediately after baking the ratio of hydrogen to ammonia is less than 0.1 and gradually increases until it may far exceed unity, at which time the apparatus must be baked again. Although hydrogen interferes with adsorption of ammonia its presence is no obstacle to a proper understanding of the experiments. The partial pressure of ammonia in the experimental mixtures was estimated from the combined readings of the mass spectrometer and the ion gauge, assuming[19] an ionization cross-section for NH_3 of $3.54 \times 10^{-16} cm^2$. Pressures measured this way are inherently inaccurate, and the real pressures of ammonia near the crystal and far away from the ion gauge and mass spectrometer were probably somewhat different. Calculated values of exposure to ammonia in these experiments therefore are liable to error and are only approximate.

Admission of ammonia proved difficult because of strong physical adsorption on the apparatus walls, as has also been

found by others.[10,18,20] When the ammonia valve is opened the partial pressure of ammonia at the mass spectrometer shows no significant increase for many minutes, and only after hours does the gas mixture of ammonia, nitrogen and hydrogen reach equilibrium at a steady flow. Extremely sluggish behavior is found also when one closes the ammonia valve, several hours being necessary to pump down to 10^{-9} torr. Ammonia is then desorbing from the walls which are now a source of ammonia, rather than a sink as during admission.

Because of the awkwardness of admitting and pumping out ammonia, experiments have been conducted in a flow system in which the equilibrium partial pressure of ammonia is conveniently small. In most cases the ammonia pressure was in the range 10^{-9} to 10^{-7} torr, but in some experiments pressures in the 10^{-6} torr range were used. During flash heating the times were always kept short compared with the impingement rate of ammonia so that very little ammonia struck the crystal while it was hot. Ammonia was adsorbed at room temperature in all of the experiments described here.

Isotopic ammonia (99 At. per cent ^{15}N from Volk Radiochemical Co.) was used rather than ordinary ammonia. Decomposition of ammonia gave $^{30}N_2$ so that any contamination by ^{28}CO was readily detected in the mass spectrometer. Adsorbed CO was not present in appreciable amounts in any of the experiments, and in a flashoff, CO never exceeded 1 per cent of the $^{30}N_2$. Apparent pumping speeds for nitrogen and hydrogen were measured by admitting these gases

to 10^{-6} torr with the pump off, then measuring the time constant of evacuation when the pump was turned on. This method simulated to a good approximation a pressure burst to the pump during a flashoff. Apparent pumping speeds were somewhat lower than the rated values for equilibrium flow.

During adsorption experiments the only ambient gases detected in significant amounts were ammonia, nitrogen and hydrogen. A mass spectrum of a typical gas mixture after long times of ammonia flow is shown in Fig. 1. The peaks at m/e = 18 and m/e = 17 are due to $N^{15}H_3^+$ and $N^{15}H_2^+$ which are expected in about equal proportions.[21] They are much larger than the $N^{15}H^+$(m/e = 16) peak.

I. FLASH DESORPTION MEASUREMENTS

Some preliminary measurements of the adsorption of nitrogen and hydrogen were found necessary, but most of the work reported here is flash off after ammonia adsorption.

Adsorption of Hydrogen and Nitrogen

Hydrogen at about 5×10^{-8} torr was adsorbed on the clean surface and flashed off after various exposures. Typical desorption spectra are shown in Fig. 2 after exposures of 0.6×10^{-6} torr-sec (0.6 L), 3 L and 12 L*. After 12 L exposure there are two clearly defined pressure maxima at about 400°K and 600°K labelled α and γ. The possible presence of a third peak β is inferred from the shape of the high temperature tail and is sketched in as a dotted line. The γ peak develops first with

* This abbreviation is used throughout this paper.

sticking probability 0.3, in good agreement with Armstrong's estimate.[22] Only when the γ coverage is near its saturation value do peaks α and β appear. This is shown in the graph of Fig. 3.

Maximum coverage of hydrogen in peak γ is about 8×10^{14} molecules cm^{-2}, which is about the number of tungsten atoms per cm^2 in a (211) plane (8.19×10^{14}). If the hydrogen is dissociated there are then about 2 monolayers of H atoms in a complete γ layer. We estimate the average heat of adsorption of γ hydrogen to be about 38 kcal/mole, using the method of analysis of Redhead[23] and assuming second order desorption kinetics.[24-26] This is to be compared with a value of 46 kcal/mole reported by Rootsaert, van Reijen and Sachtler[27] for W(211), and values near 35 kcal/mole reported for polycrystalline tungsten.[24-26]

Recently, Mimeault and Hansen[26] have shown that on polycrystalline W, hydrogen is adsorbed as atoms in a primary layer and as molecules in a more weakly held second layer. It is likely, therefore, that α and β hydrogen on W(211) are both molecular, with a combined coverage of about 1 monolayer of molecules.

In the studies of nitrogen adsorption (from Volk Radiochemical, 99 atomic per cent ^{15}N) the background pressure of hydrogen was always rather large and reliable values for maximum coverage were not obtained. Chang has, however, reported a flashoff of about 6×10^{14} molecules of nitrogen per cm^2 at saturation.[28] We find that nitrogen desorbs in a pressure burst

at high temperature, and desorption is most rapid at about 1200°K. A weakly held γ state as found by others on polycrystalline tungsten was not detected in our tests.

Gas phase hydrogen strongly retards adsorption of nitrogen at room temperature, and even a small percentage of hydrogen in the nitrogen can lead to a serious reduction of the sticking probability. However, with the crystal steadily heated at 850°K rather than at room temperature, the sticking probability of nitrogen is considerably enhanced. At this temperature the surface is kept free of adsorbed hydrogen and adsorption of nitrogen is no longer hindered by blocked sites. Such a retarding effect of hydrogen on nitrogen adsorption at room temperature has already been clearly demonstrated for polycrystalline tungsten[29,30] and hence may be important for planes other than (211) as well.

Adsorption of Ammonia

Although ammonia, hydrogen and nitrogen can individually be adsorbed upon a tungsten crystal surface at room temperature, the constant presence of the last two of these gases in our chamber does not seriously interfere with our ability to study ammonia adsorption by itself. The reasons for this are the facts that at room temperature the effective sticking probability of nitrogen in the presence of hydrogen is so much lower than that of either of the other two gases that it does not interfere detectably, and that hydrogen which is adsorbed initially is eventually completely replaced by ammonia after a sufficiently

long exposure. (See also Estrup and Anderson.[18]) Also nitrogen does not interfere with ammonia adsorption at room temperature on polycrystalline tungsten.[4,5,9,31] On W(211) this simplicity is probably true only at room temperature. At elevated temperatures serious and confusing interference from strongly held nitrogen is to be expected.

This replacement of hydrogen by ammonia is illustrated by the flash-off curves of Figs. 4 and 5. In Fig. 4 is shown the hydrogen evolved as the crystal was heated rapidly to high temperature after an initial moderate exposure to an ammonia-hydrogen mixture. No nitrogen is evolved at low temperature (i.e. no A peak for nitrogen). All of the nitrogen appears as a pressure burst at the high temperature of the hydrogen B peak. In Fig. 5 are shown low temperature sections of curves similar to Fig. 4 obtained after exposures for different times -- 0.5, 1.0 and 2.0 minutes at ammonia pressure of 1.0×10^{-7} torr. After sufficiently long ammonia exposure (12L) the A_2 peak is no longer present, and the A_1 peak is increased in size (as well as the B peaks of both hydrogen and nitrogen, not shown).

An important inference is to be drawn from this experiment, namely that ammonia adsorbed at room temperature is undissociated. If it were dissociated, adsorbed atoms from hydrogen would be indistinguishable from H atoms from dissociated ammonia and only a single peak at 600°K would be expected. (Compare Fig. 2). Growth of peak A_1 from ammonia, as the hydrogen peak A_2 disappears with increasing exposure, is evidence that hydrogen

coadsorbed with ammonia is gradually replaced by ammonia from the gas phase if the exposure is long enough. Evolution of hydrogen at 500°K in peak A_1 is therefore the result of partial decomposition of NH_3 at that temperature to give hydrogen and a strongly held residue. This conclusion that at room temperature ammonia is adsorbed without decomposition is confirmed also by work function measurements described later in Section III.

The basic fact that the A_2peak is produced by directly adsorbed hydrogen was readily established by flowing extra hydrogen into the chamber with a pre-set steady flow of ammonia. If one maintains constant the total gas pressure, ammonia plus hydrogen, then this change to an increased precentage of hydrogen gave always an increase of the A_2 peak and partial suppression of other peaks. (e.g. Fig. 5). When, however, the ammonia exposure is kept constant for different hydrogen pressures, one obtains the results of Fig. 6. In this figure are plotted flash-off measurements obtained after constant ammonia exposure of 3.5L, with different amounts of added hydrogen to vary the ammonia hydrogen pressure ratio in the range between 0.001 and 4. Separate curves show the amounts of hydrogen in the A_1, A_2 and B peaks, and also the amount of nitrogen flash-off in the B peak (at about 1200°K also).

One can judge ammonia coverage from the flash-off of the ammonia residues represented in Fig. 6 by the B hydrogen peak and the B nitrogen peak. The ratio of these curves is always

about 2 which indicates that the residue is NH_2. There is no evidence here, or in any other of our experiments, of further decomposition to give adsorbed NH or of evolution of NH_2 not completely broken down to nitrogen and hydrogen.* (See also Estrup and Anderson.[18])

The retarding effect of hydrogen on ammonia adsorption is shown in Fig. 6 by the 5-fold decrease in the amount of adsorbed ammonia after 3.5 L exposure as the admixture of hydrogen is increased to its highest value. One judges that this retarding effect should become negligible just when there is no A_2 hydrogen flash off, at $p_{NH_3}/p_{H_2} \sim 4$. At this point the A_1 flash-off peak represents just half the amount of hydrogen in the B hydrogen peak and thus accounts for the hydrogen atoms removed at 500°K from adsorbed NH_3 to leave the NH_2 residues. The collision rates of our isotopic ammonia and hydrogen molecules become equal when the ratio of their pressures is 3, and one notes that at this ratio the retarding effect of hydrogen is quite small. This implies fast replacement of adsorbed hydrogen by NH_3, a high sticking probability for NH_3, and lower sticking probability for hydrogen; a value of 0.8 for ammonia is deduced below, in satisfactory agreement with 0.45 reported by Estrup and Anderson[18] on clean (100) tungsten, and the value of 0.3 for hydrogen was reported above. The hydrogen A_1 peak is

---

* One notes that Melton and Emmett[32] observed minute quantities of evolved NH and NH_2 radicals from surfaces of platinum and iron, but in amounts far too small to be detectable in our apparatus.

properly stoichiometric with the B peaks of hydrogen and nitrogen only when there is no significant hydrogen adsorption, i.e., no A_2 peak. Only then is the hydrogen of the A_1 peak just equal to half that of the B hydrogen peak as required to account for all the atoms in NH_3. At lower values of the ammonia/hydrogen gas pressure ratio the A_1 peak is too large. This suggests that the A_2 peak "feeds" the A_1 peak, with some association of adsorbed hydrogen atoms with NH_2 leading to an evaporation route via NH_2 fast enough to compete with normal evaporation of ordinary hydrogen at the higher temperature of 600°K.

For convenience we represent the amounts of hydrogen in the flash-off peaks by the letters identifying the peaks. With this nomenclature the fraction of "extra" hydrogen in the A_1 peak is $(1 - 0.5\ B/A_1)$. In Fig. 7 this fraction is plotted against the number of hydrogen molecules in the B peak. From this plot the number of H_2 molecules in the B peak is about $1.3 \times 10^{15} cm^{-2}$ for the exposure 3.5 L when there is no interference from adsorbed hydrogen. From kinetic theory the number of molecules of NH_3 at 300°K reaching the surface for an exposure Q measured in L units is $4.8 \times 10^{14}\ Q\ cm^{-2}$, or 1.7×10^{15} for exposure 3.5 L. The indicated sticking probability for NH_3 is 0.8 in the absence of hydrogen.

Complete NH_2 Coverage

We have shown that complete coverage of NH_3, that is without uncombined hydrogen, is attained by long exposure permitting

NH_3 to replace initially adsorbed hydrogen. But maximum NH_2 coverage is not attained by flashing such a saturated surface to about 800°K. This is found out by observing that, after further exposing such a surface to NH_3, a second flash to 800°K evolves additional hydrogen in an A_1 peak, and of course an enhanced B peak upon complete cleaning. This is taken to mean that adsorbed NH_2 radicals are smaller than adsorbed NH_3 molecules.

Maximum NH_2 coverage is attained by several exposures with intermediate heating to 800°K. In Figs. 8 and 9 are shown flash-off observations after 1, 2 and 3 exposures of 90 L each with intermediate heating to 800°K. Relative values of numbers of molecules arriving at the mass spectrometer are marked on the peaks in the figures. The integrated numbers of molecules of hydrogen and of nitrogen in the different flash-off peaks are collected in Table I, and for comparison theoretical values calculated from the LEED measurements of Section II. The agreement is good in view of uncertainties in our flash desorption measurements. From the flash-off numbers one estimates the area occupied by an NH_2 radical to be 4.8 Å.^{2} This is in quite satisfactory agreement with a theoretical value of 5.45 Å^2 obtained from the structure found in Section II for NH_2 radicals packed together at maximum density.

Desorption of Molecules and of Atoms

The hydrogen atomization experiments of Brennan and Fletcher[33] and of Hickmott[24] lead one to expect that atomic hydrogen might be desorbed when NH_2 is decomposed at 1200°K.

We have some strong circumstantial evidence that this may be so, with H atoms combined into molecules on the walls of the chamber before they reach the mass spectrometer located in a side arm. Our available evidence suggests, however, that the nitrogen from NH_2 leaves the surface as molecules, as does the hydrogen of the A_1 peak.

Desorption curves for hydrogen and nitrogen, measured in the mass spectrometer as H_2 and as N_2, are superposed in the lower half of Fig. 10. The surface before the flash-off had been completely covered by NH_2 by the method of alternate exposure and low temperature flash as described above. Not only does the maximum in the hydrogen trace come <u>after</u> that of nitrogen, but also there is a long tail on the hydrogen trace which is lacking in the nitrogen trace. This is more obvious in the upper box of Fig. 10, which shows the integrated number of hydrogen and nitrogen <u>molecules</u> sensed at the mass spectrometer. We suggest that hydrogen reaches the mass spectrometer later than nitrogen because it leaves the crystal as atoms which linger on the walls of the chamber until they are combined there into molecules.

We report another observation supporting this speculation. We have pointed out above that all experiments were carried out in a stable steady flow of ammonia, with its accompanying hydrogen and nitrogen. In general, steady flow had been maintained for many hours with the walls of the chamber in equilibrium with this flowing gas mixture. When we have

deviated from this situation and carried out a test after the chamber was freshly baked and its walls not in equilibrium with the gas, peak A_1 hydrogen and peak B nitrogen were found just as if the apparatus had been "aged" in flowing ammonia for several days - but peak B hydrogen was not detected at all. It could be found, although still small, in a second experiment after the lapse of one hour, and aging for more than one day was necessary for peak B hydrogen to become stoichiometric with peak B nitrogen. We interpret these results to mean that nitrogen and low temperature hydrogen desorb as molecules, but high temperature hydrogen desorbs as atoms; these H atoms stick to the walls if the walls are clean, but if the walls are in equilibrium with the flowing gas they soon recombine and leave as molecules. The inference is that strongly held NH_2 decomposes at high temperature to eject H atoms and leave mobile adsorbed N atoms; these immediately combine and are at once desorbed as molecules.

Change with Coverage of NH_2 Bond Strength to the Substrate

We have evidence that the strength of the NH_2 bond to the substrate is a function of coverage, with the strength weakest at complete coverage. This effect is apparent in Figs. 8 and 9 where the B peaks, for both hydrogen and nitrogen, occur at lower temperatures for the higher coverage. Data collected for the complete range of NH_2 coverage are exhibited in Fig. 11(b).

In a modified experiment we measured in a series of tests the temperature at which the hydrogen of the B peak just starts to desorb. At the beginning of the experiment a complete NH_2 layer was formed, in the usual way by repeated exposures with intermediate heating to 800°K. This complete layer was then flashed to an experimental temperature (abscissa of Fig. 11(a)) above 800°K and then given a long room temperature exposure of NH_3 before flashing to the next higher temperature. The temperature at which hydrogen of the B peak just began to desorb in each case is plotted in Fig. 11(a) against the experimental maximum temperature to which the crystal had been flashed just before. This temperature of the beginning of the hydrogen flash-off is observed to be lowest for the largest amount of NH_2 coverage, in agreement with the measurements upon the maximum of the flash-off (Fig. 11(b)).

II. DIFFRACTION MEASUREMENTS

The orientation of the W(211) surface relative to the beam for all the LEED patterns in this section is shown in Fig. 12. We need to specify this orientation because there is only one mirror plane perpendicular to the surface, as can be seen from the ball model. In some experiments the crystal was mounted with the [1$\bar{1}\bar{1}$] direction pointing down rather than up, and photos of LEED patterns from this crystal have been rotated 180°so that all the LEED patterns can be compared easily.

The most striking feature of the (211) surface, which is the third densest face of tungsten, is its furrowed nature. Troughs lie between close packed rows of W atoms and give the surface something of a one-dimensional character. This structural feature has a decided influence on the nature of the NH_2 structures that are formed by thermal decomposition of adsorbed NH_3.

Adsorption at Room Temperature

In Fig. 13 are compared LEED patterns produced by hydrogen and ammonia adsorbed at room temperature and not subsequently heated. There are no fractional order beams, and all the patterns are (1x1) with low background. Relative beam intensities are not seriously affected by adsorbed hydrogen but are quite markedly changed by adsorbed ammonia. At the present state of the art, little can be deduced from the LEED intensities concerning the surface positions of adsorbed H atoms from hydrogen adsorption, or positions of adsorbed NH_3 molecules after ammonia adsorption. We can infer from Fig. 13 that the unit meshes of H-covered and NH_3-covered W(211) surfaces have the size shown in Fig. 12, and that these surfaces contain an integral number of monolayers of H atoms or NH_3 molecules (defining 1 monolayer as the number of W atoms in a (211) plane).

Heating the hydrogen-covered surface causes no change from (1x1) symmetry. The pattern simply becomes a (1x1) clean surface pattern after all the hydrogen is off the surface at

low temperature (Fig. 2). But great changes can be produced by heating an ammonia covered surface.

Thermally Ordered NH_2

After the low temperature hydrogen (peak A_1) is driven off by heating to about 700°K (Fig. 8) the background in the LEED patterns increases considerably, indicating a disordered arrangement of NH_2 radicals on the surface. The patterns are, however, still (1x1). Heating to higher temperatures causes the NH_2 radicals to become well ordered with no further gas evolution. The resulting C(4x2) structure is described below.

Development of this C(4x2) structure is shown in Fig. 14. The photographs of Fig. 14a, b and c were obtained after single saturation doses of ammonia and then heating respectively to 750, 800 and 850°K. Evidently degree of ordering after single doses depends on the flash temperature, and 850°K is sufficiently hot to effect good ordering of the NH_2 groups. The patterns of Figs. 14d and 14e were obtained after multiple saturation doses of NH_3 separated and followed by flashing at 875°K, Fig. 14d after two doses and Fig. 14e after three. It is evident from Figs. 14c, d and e that redosing causes virtually no changes in the relative intensities of diffraction beams from the C(4x2) structure. This is taken to mean that redosing merely increases the coverage of C(4x2) and does not change the structure by forming, for example, a second layer of NH_2. This is consistent with creation after 1 dose and low temperture flashing of regions where the NH_2 C(4x2) structure is

well developed, as well as regions thought to be bare giving a (1x1) pattern. Formation of such "islands" means strong lateral attractive forces between NH_2 groups in the C(4x2) layer. Redosing experiments can thus be explained by adsorption of NH_3 in (1x1) regions only. Eventually saturation coverage of NH_2 is attained and more redosing causes no further addition to the C(4x2) coverage. This is the conclusion that was reached in the flash-off experiments described earlier.

NH_2 at Reduced Surface Density

The C(4x2) structure contains the maximum NH_2 density. Structures of slightly lower density are produced by heating above 900°K. This heating causes some of the NH_2 to evaporate as nitrogen and hydrogen, and when the temperature has reached 1050°K, about 89 percent of the original NH_2 is still on the surface. Whether or not the hydrogen evaporating in this restricted temperature range is atomic we cannot say. We have already inferred from the flashoff data that the major fraction of the high temperature hydrogen is atomic, but this might not apply to decomposition below 1050°K. A reason for believing that hydrogen desorbing below 1050°K is molecular will be given later in the Discussion.

In this temperature range 900-1050°K a remarkable series of structures is found when a C(4x2) surface (redosed or not) is flashed progressively hotter. Heating the C(4x2) structure to about 1000°K causes evolution of a small amount of nitrogen

and hydrogen and a change of structure to C(10x2). This new structure gives LEED patterns shown in Fig. 15. As in the case of C(4x2), the effect of redosing and flashing to the proper temperature is not to change relative intensities but only to increase the overall sharpness and brightness of the patterns (Fig. 15b). In other words, the structure is determined solely by the maximum temperature to which the crystal has been flashed. If only one dose is given at room temperature and the crystal then heated to 1000°K, some parts of the surface are then presumed covered with C(10x2) structure and other parts are presumed to be bare, just as in the case of C(4x2). Redosing and reheating to 1000°K increases the fraction of the surface covered by the C(10x2) structure, which is 7 percent less dense than the C(4x2) structure. (See below.)

It is obvious by comparing Figs. 14 and 15 that in the C(10x2) structure the surface spacings parallel to the $[1\bar{1}\bar{1}]$ direction have changed from those in C(4x2), but that spacings parallel to the $[01\bar{1}]$ are still the same as in C(4x2). In going from C(4x2) to C(10x2) there has been an expansion of the NH_2 structure in the $[1\bar{1}\bar{1}]$ direction, along the furrows that are so prominent in the model of Fig. 12. This expansion is not, however, simply a sudden change to C(10x2) as the crystal is heated. Rather, it appears to be continuous, and a whole family of related structures is found in the temperature interval 900-1050°K. The C(4x2) and C(10x2) structures are merely two members of this family. They give LEED patterns

of high symmetry, but most of the structures in the family do not. In Fig. 16 is shown a selection of patterns obtained after the C(4x2) structure had been heated to progressively higher temperatures. Each heating to a higher temperature caused desorption of a small amount of nitrogen and hydrogen and the corresponding expansion of the NH_2 structure in the $[1\bar{1}\bar{1}]$ direction.

The patterns of Fig. 16 are generally very complicated. Nevertheless we have succeeded in interpreting all of them in terms of a continuously expanding layer of NH_2 radicals lying above the (undisturbed) tungsten (211) surface, with this layer becoming progressively more dilute with the evaporation of more and more nitrogen and hydrogen. The layer is always a simple centered rectangular mesh, no matter what the extent of its expansion in the $[1\bar{1}\bar{1}]$ direction. Complexity of the LEED patterns is due to multiple scattering of the beam between overlayer and substrate, and not to structures which are inherently more complicated.

Structures of the NH_2 Layer

To understand the diffraction patterns of Fig. 16, we analyze first the simple C(4x2) pattern of Fig. 14e. A schematic diagram of this pattern is given as Fig. 17. Beams arising from multiple diffraction between the NH_2 overlayer and the substrate are shown as light crosses, while the primary overlayer beams and primary substrate beams are indicated respectively as crosses-in circles and filled circles.

Primary beams from the centered overlayer (crosses-in-circles) are at the 3m/4, 3n/2 positions (referred to the substrate pattern) with m + n even. The integers m and n are the Miller indices of the overlayer itself. For simplicity consider double scattering, once by the overlayer and once by the substrate, because double scattering alone can give in principle all the reflections indicated by the light crosses in Fig. 17. The positions of these are given[34] by the Miller indices hk (referred to the substrate) with h = p + 3m/4 and k = q + 3n/2 where pq are indices of a substrate reflection. For example, the beam 1/4 $\bar{3}$/2 indexed in Fig. 17 could arise from a combination of the substrate 10 and overlayer $\bar{1}\bar{1}$ beams (p = 1, q = 0, m = -1, n = -1) or from the substrate 1$\bar{3}$ and $\bar{1}$1 beams, or from several other low order combinations. Referring back to Fig. 14e one notes first of all the great intensity of the $\bar{3}$/4 $\bar{3}$/2 beam (i.e., the $\bar{1}\bar{1}$ beam of the overlayer) and then the correspondingly bright beams at 10 and 1/4 $\bar{3}$/2, in good agreement with our assignment of the primary beams. One also notes the marked asymmetry of the intensities in the [1$\bar{1}\bar{1}$] direction and the presence of only one mirror plane in the pattern, which is proof that the substrate asymmetry (Fig. 12) plays a major role in determining the relative intensity of multiple diffraction beams.

The patterns of Fig. 16a-h are produced also by multiple diffraction, but with the overlayer becoming more and more expanded in the [1$\bar{1}\bar{1}$] direction, as already described.

Positions hk of multiply scattered beams in all of these patterns can be expressed by the formulae $h = p + \alpha m$ and $k = q + 3n/2$, with $m + n$ even because the overlayer is always a simple centered mesh. The quantity α changes with expansion of the overlayer, and is the quotient of the separation between substrate W atoms in the $[1\bar{1}\bar{1}]$ direction (i.e., $3^{\frac{1}{2}}a_o/2$ and the separation between NH_2 groups in the same direction. For most of the patterns of Fig. 16, the quotient is not a simple fraction. When the α is a ratio of small integers, the overlayer and substrate are in registry every few spacings in the $[1\bar{1}\bar{1}]$ direction, but when α is not such a ratio, the combined meshes are in registry only very infrequently. With α a ratio of small integers, the LEED patterns are relatively simple and have high symmetry. On the basis of our model only four simple patterns are expected within our range of expansion. They are C(4x2), P(7x2), C(10x2) and P(3x2), with respective α values of 3/4, 5/7, 7/10 and 2/3. No other patterns are expected, and none are found, for which α is a quotient of integers smaller than eleven. Patterns for P(7x2) and C(10x2) are shown in Fig. 16c and 16f.

The structures C(4x2), P(7x2), C(10x2) and P(3x2)inferred from the LEED patterns are shown in Fig. 18. The open circles represent NH_2 groups in the overlayer and the filled circles W atoms in the top layer of the (211) surface. The effect of expansion parallel to $[1\bar{1}\bar{1}]$ is very striking, and in each case we show a particular plausible placing of the overlayer

upon the substrate, chosen from placements that differ by translations parallel to the surface. (The actual placement cannot be deduced here because LEED intensities, which are affected by the placement, cannot at present be analyzed on account of lack of theory). The smallest repeating mesh of combined overlayer and substrate is a centered mesh when the denominator of the fraction α is even, and is a primitive mesh when it is odd.

The structures of Fig. 18 are compared in Table II. The centered rectangular unit mesh at any point of expansion of the NH_2 overlayer has the dimensions

$$(1/\alpha)(3^{\frac{1}{2}}a_o/2) \quad \text{by} \quad (2/3)(2^{\frac{1}{2}}a_o)$$

where a_o = 3.16 A is the cube edge of tungsten. The number Θ of monolayers of NH_2 is always 3α. A complete layer of the C(4x2) structure has a theoretical coverage of 9/4 which, if thermally destroyed, would lead to evaporation of 0.92×10^{15} molecules of nitrogen per cm^2. Comparison of these numbers with the experimental values for a redosed surface (Table I) shows an excellent agreement that is well within experimental error. This supports the model structures of Fig. 18 and is a good indication that the assignment of the positions of the primary overlayer beams in the diffraction patterns is correct.

The data of Table II have been tabulated for cases in which α is a ratio of integers smaller than eleven. We have,

however, analyzed all the patterns of Fig. 16 (as well as many others) and have determined corresponding values of α as the temperature was raised and the NH_2 coverage reduced. These values, given in the plot of Fig. 19, were obtained from two different sets of measurements of the positions of diffraction spots in the photographs. The apparently continuous decrease in α with increasing temperature means that any stage in the expansion could probably be observed. The coverage θ (equal to 3α) and the unit mesh edge of the overlayer parallel to the $[1\bar{1}\bar{1}]$ direction ($3^{\frac{1}{2}}a_o/2\alpha$) are indicated on the right hand ordinate.

The experimental points of Fig. 19 were obtained by starting with a repeatedly redosed surface having the C(4x2) structure. The crystal was then flashed for a second or two to the temperature of the abscissa, then allowed to cool and a photograph of the pattern obtained. The ammonia pressure was of the order of 10^{-8} torr. After waiting for readsorption of more NH_3, the crystal was flashed again to a different temperature, either higher or lower than the preceding flash, and another photo taken. Values of α so obtained were independent of the temperature of the preceding flash and determined only by the temperature of the last flash. Thus it is possible, with redosing to go from, say, a C(10x2) to a C(4x2) structure and back and forth as many times as desired. Evidently, the state of expansion of the overlayer from an initial C(4x2) structure

is a function of the last flash temperature only.

The fact that a high temperature (850°K) is required to order NH_2 groups into a uniform C(4x2) structure is proof that they are effectively immobile on the surface. This immobility, we believe, can give a satisfactory explanation for the observation that heating of NH_2 overlayers results in less and less dense structures rather than islands of compact C(4x2) structure. An important cause of immobility of NH_2 in these structures is the assumed strong lateral attractive forces within the overlayer which effectively prevent diffusion of the NH_2 groups. That is, only by a cooperative motion of all NH_2 groups could a whole structural region shrink by evaporation and maintain a C(4x2) structure (providing that evaporation from island edges is ruled out). Such cooperative motion is highly unlikely, and one therefore infers that evaporation proceeds in such a way as to maintain a uniform distribution of NH_2 over regions of essentially unchanging area, i.e., dilution of the overlayer as we have described. We also point out that development of islands of NH_2 after a single dose of ammonia and heating to 500°K does not require long range mobility of NH_2, but is expained by diffusion of NH_3 and decomposition of the NH_3 at the edges of disordered islands of NH_2. Heating then orders such islands but with difficulty owing to the strong forces between the NH_2 groups, and even at 750°K ordering is not yet complete (Fig. 14a).

An alternative explanation of why heating NH_2 overlayers does not create islands of compact C(4x2) structure is that the proportions evaporating of nitrogen and hydrogen may not be in the ratio 1:2. This would mean the surface stoichiometry would be a function of α and that the real structures on the surface would be more complicated than those already deduced. Careful checks of stoichiometry of the desorbing gases in the range of expansion from C(4x2) to P(3x2) have not been made, which in any case would be extremely difficult in view of the small amounts of desorbate. For the present we assume that NH_2 is the only surface species in this range of coverage.

Although the amounts of hydrogen and nitrogen evolved during the transitions between the different structures are small and have not been measured with great precision, those measurements that have been made do agree within experimental error with values calculated from the structures. Measured values for hydrogen evolution are given in Fig. 20, expressed as fractions of the total hydrogen contained in the original C(4x2) structure. In each case the starting surface before flashing was saturation coverage after a single dose of ammonia. The temperatures at which P(7x2) and C(10x2) are formed are marked by arrows; for these the theoretical fractions are respectively 0.049 and 0.067 (Table II). The theoretical fraction for the P(3x2), which is never quite reached, is 0.11.

One might expect unusual stability for those surface structures for which the epitaxial relation with the substrate is simple.[35] That this is true is evident in the case of the

C(4x2) structure which is stable over a considerable temperature range before suddenly changing at about 900°K. It seems to be even true to a lesser extent for the C(10x2), judging from the shape of the curve of Fig. 19.

Proposed Locations of Hydrogen Atoms

The C(4x2) structure of Fig. 18 is reproduced in Fig. 21 with added details showing N and H atoms drawn to scale with their accepted covalent radii of 0.75 and 0.37Å. If this structure is correct, the H atoms are shared by the N atoms in a way analogous to hydrogen bonding, but with the N...H...N bonds stronger than normal and considerably shorter (2.35Å) than the usual distance[36] of 3.1Å. The obtuse angle HNH in these structure is similar to the angle HNH = 103° of the bent ground state of the amidogen radical (NH_2) in the gas phase.[37] In Table III are collected the values that we infer for the N...H...N distances and the obtuse angles HNH for the range of structures from C(4x2) to P(3x2).

There are other interesting attributes of this model. It is expected theoretically that each H atom should move in a single potential well centered on a point midway between nitrogen atoms if the N...H...N distance is small, but if the N...H...N distance is greater a double minimum in the potential is expected. This has very recently been calculated by Sabin[38] for N...H...N bonding in a pyridine-pyridinium complex. His calculations show that a double minimum first appears for an N-N separation of 2.2Å. At an N-N separation of just 2.35Å

(first entry in Table III) the calculations indicate a hump between minima of height about 8 kcal/mole, rising to about 20 kcal/mole for a separation of 2.53Å (last entry in Table III). Although the absolute values of these barrier energies are not too reliable[39] they are of the proper order of magnitude. Clearly in the C(4x2) structure the H atoms are localized about halfway between N atoms, as shown in Fig. 21, but as the overlayer expands to stretch the N...H...N bonds, the H atoms begin to oscillate back and forth across the potential hump between the N atoms. By the time the P(3x2) structure is reached these oscillations (which may or may not be coupled with each other) are so disruptive that the overlayer becomes unstable. It is then changed drastically into what we call the "pseudo-N" structure. We believe that the NH_2 groups are then bonded to the substrate in essentially the same way as are N atoms after adsorption of pure nitrogen. Presumably a hydrogen-bonding type of interaction plays little or no role in the bonding in the "pseudo-N" structure.

Uniqueness of Surface Structures

Some consideration must be given to the possibility of accounting for the C(4x2) diffraction pattern (Fig. 17) by a structure differing from that sketched in Fig. 18. C(4x2) patterns can be produced (by multiple scattering) for any centered rectangular overlayer having unit mesh dimension parallel to $[1\bar{1}\bar{1}]$ of $(3^{\frac{1}{2}}/2)a_o/(\frac{1}{4} + \frac{r}{2})$ and unit mesh dimension parallel to $[01\bar{1}]$ of $2^{\frac{1}{2}}a_o/(\frac{1}{2} + s)$, where r and s are

positive integers including zero. In the C(4x2) structure of Fig. 18, r = s = 1, and the question we must examine is whether another choice of r and s would not be equally reasonable. We will give arguments here to support the structures already deduced.

One can show that if r is even the sequence of diffraction patterns for an expanding overlayer* is not C(4x2), P(7x2), C(10x2), P(3x2) but a completely different sequence. Hence r must be an odd integer. During expansion of the overlayer the field of intense diffraction spots is always dense, hence α is restricted to small values. Since α for C(4x2) is equal to $\left(\frac{1}{4} + \frac{r}{2}\right)$, this means small values of r with r odd. Possible values are r = 1 or r = 3. If r were as great as 5, the overlayer would have to be compressed to a physically impossible degree parallel to $[1\bar{1}\bar{1}]$.

Next we consider possible values of s. We have already assumed that s remains unchanged during expansion of the overlayer, i.e., there is expansion only along the troughs of Fig. 12. Limitation on the magnitude of s is obtained from considerations of coverage, and it is easily found that there are only two reasonable possibilities to be considered for r and s that could give the experimental flash-off results.

---

* It is very unreasonable to postulate a structure becoming ever denser as overall coverage is reduced, because this would require formation of islands more and more concentrated in NH_2, as well as creation of areas of clean surface.

These are r = s = 1 considered already, and r = 3, s = 0 which we will now consider and then reject.

The C(4x2) structure for r = 3 and s = 0 is sketched in Fig. 22. One attractive feature of the C(4x2) structure of Fig. 22 is the packing of NH_2 groups (small circles in the figure) within and along the troughs of the substrate. The separation of NH_2 groups along the troughs is just $(4/7)(3^{\frac{1}{2}}/2)a_o$ = 1.57Å, which is quite close to the covalent diameter of a nitrogen atom. On this model hydrogen bonding does not occur, and the H atoms (not shown in Fig. 22) must still be directly attached to the N atoms and not to the substrate. A second attractive feature is that the NH_2 radicals lie directly in the troughs rather then being attached together by hydrogen bonds as in the overlayer model of Figs. 18 and 21. On the other hand, the troughs in Fig. 22 are separated by the large distance 4.47Å and it is very difficult to understand why every second colum of close-packed NH_2 groups should be staggered as they must to give a centered structure. In this connection we cite Gerlach and Rhodin[40] who have recently studied adsorbed sodium on a Ni(110)surface. This nickel surface has troughs in the close packed surface direction very similar to our (211) tungsten surface, but columns of sodium atoms adsorbed in the troughs have no correlation from trough to trough. The model of Fig. 22, however, does require strict correlation between columns of NH_2 radicals, otherwise the C(4x2) pattern (and also patterns from the expanded overlayer) could not have the

strong sharp spots that they do. Such a long-range correlation seems unreasonable and argues against the model, while in the model of Fig. 21 all NH_2 groups are in mutual contact. Absence of tell-tale streaking during ordering of the C(4x2) structure (Fig. 14) also argues against the model of Fig. 22.

We next discuss surface coverage and changes of coverage during expansion of the overlayer. We have seen that the model of Fig. 21 has coverage in good agreement with the flash-off data (Table I) and that during expansion of the overlayer an appropriate amount of evolved hydrogen is detected (Fig. 20 and Table II) If, on the other hand, the model of Fig. 22 is correct the NH_2 coverage of C(4x2) would be 1.75 monolayers, falling only slightly to 1.67 monolayers after expansion into a P(3x2) structure. These numbers are in poorer agreement with experiment than those calculated from the model of Fig. 21. Also, during expansion of the overlayer of Fig. 22, the N-N distance is calculated to stretch from 1.56Å to 1.64Å, and both these distances are longer than the <u>single</u> bond length in hydrazine of 1.46Å. This is another argument against the second model.

Most of the points just raised favor the structure of Fig. 21. We next give diffraction arguments that bolster this conclusion, and we first note that in Figs. 14, 15, and 16 intensities in the column k = 3/2 are greater than for k = 1/2 and k = 5/2, supporting the assignment s = 1 rather than s = 0. In Fig. 14 the $\overline{3/4}$: $\overline{3/2}$ spot is very intense and is a primary

overlayer beam according to the model of Fig. 21. According to the model of Fig. 22, however, this could be explained as a combination (double scattering) of the overlayer $\bar{1}\bar{2}$ beam, referred to its own mesh and the substrate 10 beam. The absence of a strong spot at $\overline{3/4}\ \overline{1/2}$ in Fig. 14(e) is evidence that the structure of Fig. 22 is incorrect, because one would expect also strong intensity for the combination of the overlayer $\bar{1}\bar{1}$ and substrate 10 beams. That is, one would expect approximately equal intensities at the $\overline{3/4}\ \overline{3/2}$ and $\overline{3/4}\ \overline{1/2}$ positions of Fig. 14(e), and this is not found.

For r = 3, the diffraction "orders" required to be assigned to the overlayer scattering are generally larger than for r = 1. It is expected that multiple diffraction spots involving these high orders should be weak[41] rather than as strong as observed, though the theory of these intensities is hardly developed. In the same way that we defined α for r = 1, we can define α' for r = 3. One can show that $\alpha' = 1 + \alpha$ so that $h = p' + (1 + \alpha)m'$ for a spot hk produced by double scattering (using our previous nomenclature). Hence $m = m'$ and $p' = p - m$, and $|p'| = |p| + |m|$. Therefore beams requiring p' (structure of Fig. 22) have orders greater than or equal to those of beams involving p (structure of Fig. 21) which argues strongly against r = 3 and favors r = 1, i.e., favors the structure of Fig. 21. For example, we give in Table IV lowest order combinations for values of h in the C(10x2) pattern. The numbers p' in the last column of the table are in some cases so large that r = 3 is very

unlikely (compare intensities in Fig. 15). In Figs. 14, 15 and 16 the spots 3/2, α and $\bar{3}/2$, α are very intense for all values of α, as are also their combinations with the substrate beam 10. This is again very good circumstantial evidence for concluding that r = 1, and that the interpretation leading to the structures of Fig. 18 is basically correct. Finally, we have the observation that weak second layer adsorption of ammonia can alter relative diffraction intensities severely (Section III). The alterations of intensity are consistent with the structure of Fig. 18 rather than that of Fig. 22.

These diffraction arguments together with the other arguments we have given lead us to strongly prefer our first model with NH_2 radicals connected together via hydrogen bonds. We saw that as these bonds become stretched more and more during expansion of the overlayer, a point is reached where a hydrogen bonded layer is no longer stable. At this point there is a drastic surface rearrangement and development of what we call the "pseudo-N" structure.

"Pseudo - N" Structure

This "pseudo-N" structure that forms at 1050°K gives diffraction patterns which are very similar to those produced by adsorbed nitrogen that has been heated to the same temperature, reported by Chang.[28] The similarity is the reason for giving this name to the structure.

The "pseudo-N" structure begins to develop just at the temperature at which a P(3x2) structure would be expected on

the basis of the curves of Figs. 19 and 20. Actually, well-formed P(3x2) patterns are not observed and the transition to "pseudo-N" occurs just before the overlayer has expanded to the extent required by P(3x2). In all discussions so far, the P(3x2) structure has been invoked only for reason of helping the arguments, in spite of its not actually being found. Patterns sufficiently near to P(3x2) have, however, been detected just before the "pseudo-N" to justify inclusion of P(3x2).

Such a pattern is shown in Fig. 23A, along with a well developed "pseudo-N" pattern in Fig. 23B. Close examination of Fig. 23A shows weak spots characteristic of a structure exceedingly like P(3x2) along with other incipient features characteristic of the "pseudo-N". In this transition stage the background is very high owing to surface disorder accompanying the transformation into "pseudo-N". Some of this disorder may be connected with the evolution of considerable amounts of desorbate (see Fig. 20). We estimate that NH_2 coverage in the "pseudo-N" is about 75 percent of that in C(4x2), i.e., approximately 1.7 monolayers referred to the (211) surface. (Recall that the P(3x2) structure has a theoretical NH_2 coverage of just 2 monolayers, Table II.)

Owing to the complexity of the "pseudo-N" patterns we have not yet succeeded in deducing the surface structure and more experiments are required. There is reason, however, for believing that the "pseudo-N" surface is a faceted surface; that is, the original (211) plane has been rearranged into a

hill-and-valley arrangement of other planes covered with adsorbed NH_2 groups. The similarity of the "pseudo-N" patterns and those from adsorbed nitrogen suggests that the facets are the same in the two cases. We propose to study these two patterns further, and discussion of them which could be given at this time we postpone until more detailed knowledge is available.

An important similarity between the structures produced by N atoms and by NH_2 is the fact that both are destroyed at the same temperature to give a clean surface ($\sim$ 1200°K). This observation implies that the bonding modes as well as the surface structures, for N atoms and NH_2 groups in "pseudo-N", are essentially the same. This point is important in assessing the deductions drawn by Dawson and Hansen[16] from their field emission microscope study of ammonia on a tungsten tip. The present LEED results and those of Estrup and Anderson[18] suggest strongly that the data of Dawson and Hansen require reinterpretation. This is taken up below under Discussion.

III. SECOND LAYER ADSORPTION

When any of the well ordered NH_2 structures described above is further exposed to ammonia at room temperature the diffraction pattern becomes clouded over by a general diffuse haze arising from physisorbed NH_3 randomly held in a second layer. Many sharp features of the original pattern are unchanged, but those diffraction beams produced only by high order multiple scattering are largely eliminated. In Fig. 24 is shown the

effect of NH_3 adsorption upon a well ordered P(7x2) structure. (Note retention of low order beams appropriate to the structure of Fig. 18.) Similar effects have been observed when NH_3 has been adsorbed upon C(4x2), C(10x2) and other structures. The weakening of beams produced by high order multiple scattering, as well as the general haze, is to be expected as a result of general diffuse scattering from a second layer lacking good order.

That this effect is due primarily to physisorbed NH_3 cannot be confirmed in direct manner by flash-off measurements because changes of NH_3 pressure are buffered by the walls of the chamber as described in Section I. Measurements of changes of work function have, however, given desired information, and have yielded also data of interest for their own sake. These measurements were made with the special help of J. C. Tracy Jr.[41] using the Kelvin vibrating capacitor method. Particular care was taken to prevent thermal disturbance of the vibrating reference reed (tin-oxide coated stainless steel), and the reference reed was always moved away from the vicinity of the crystal whenever the crystal was to be flashed. Checks were made which showed that flashing the crystal below about 1800°K had no appreciable effect on the work function of the reed, providing the reed was always moved away during flashing. Tests were also made for reproducibility of work function after the reed was moved and returned to its measuring position; measurements were always reproducible to better than 100 mV.

Experiments were conducted with a continuous flow of NH_3 at low pressure in an equilibrium mixture containing some hydrogen and nitrogen as described in section I.

From curve 1 of Fig. 25 one concludes that NH_3 molecules adsorbed upon clean W(211) reduce the work function by about 0.8 volt, and from curve 3 that NH_3 upon a nearly full monolayer of NH_2 gives a reduction of about 0.9 volt. Extrapolations of curves 2 and 3 indicate that adsorbed NH_2 produces no change of work function. The results are collected in Table V, together with observations from the literature of the work function changes of (211) tungsten resulting from the adsorption of hydrogen and nitrogen.

Coadsorbed hydrogen in the first layer reduces $\Delta\phi$, as one might expect from the numbers given in Table V. Hydrogen also slows down the rate of change of $\Delta\phi$ by retarding ammonia adsorption in the first layer, which is the same result found earlier in Section I from flash-off experiments. Gas phase nitrogen evidently has no effect on the work function at room temperature because it is not adsorbed in the presence of hydrogen and ammonia. Although there is some influence of hydrogen upon the second layer adsorption that has not yet been carefully appraised, it is believed not to be serious. However, the results are extremely sensitive to CO contamination, which replaces the second layer of NH_3 with very high efficiency and causes a resulting gradual decay in the measured value of $\Delta\phi$.

The explanation of curve 1 of Fig. 25 is that ammonia molecules are adsorbing undissociated on the bare W(211) surface

with the lone pair of electrons pointing down into the surface. Evidently lowering of ϕ is a simple consequence of the permanent dipole moment of the NH_3 molecule of 1.5 D, and therefore it is very probable[44] that the bonding is essentially of the Van der Waals type. Heating causes development of NH_2 structures and evolution of hydrogen (section I), and ϕ changes to a value expected from a covalent type of bonding. Molecules of NH_3 in a second layer are then held to the NH_2 layer by Van der Waals attraction, and again the permanent dipole moment of the NH_3 molecule explains the fall of ϕ in curves 2 and 3 of Fig. 25.

The experiment was continued as shown in Fig. 26. The first three points of Fig. 26 are taken from the curves of Fig. 25 and the other points from similar curves as the experiment progressed. The work function change produced by NH_2 layers is essentially 0.0 eV, hence the changes in ϕ shown in Fig. 26 are probably due entirely to NH_3 molecules. For example, flashes 4-9 show that a layer of NH_3 on a saturated sublayer of NH_2 lowers ϕ by about 0.9 eV. This is a smaller change than after flash 2, and the explanation may be depolarization within the second layer. Flashes 10-13 demonstrate that second layer NH_3 molecules are thermally quite labile and desorb readily at low temperatures, as expected for a Van der Waals type of binding.

DISCUSSION

The importance of adsorbed NH_2 radicals as intermediates in the decomposition of ammonia on metal surfaces has long been recognized,[6,10-15, 18,20,45-50] but unfortunately in many cases

it has not been possible to decide whether or not further dissociation to NH or even N actually occurs. Though adsorbed NH radicals in particular have often been invoked in ammonia decomposition studies, proof of their existence often has not been convincing. It is, therefore, of considerable interest that Nakata and Matsushita[51] have recently discovered from IR studies that NH_2 radicals are formed after exposure of an iron surface to NH_3.

Recently, Estrup and Anderson[18] in their study of decomposition of NH_3 on a W(100) surface, stated that only NH_2 radicals were formed with no evidence for dissociation to NH or N. In the present work on W(211), we draw the same conclusion. We point out, however, that false deductions concerning the surface radicals can easily arise, e.g. interpretation of Fig. 6 is made more difficult due to coadsorption of hydrogen when the hydrogen partial pressure is large, and only a full accounting for all desorbed species can allow proper conclusions to be drawn.

The question of whether or not NH_2 breaks down to imino radicals or to adsorbed N atoms is fundamental to a correct understanding of ammonia reactions on metal surfaces. It has very recently been claimed by Dawson and Hansen,[16] from their field emission study of ammonia adsorption and decomposition on a W tip, that complete dissociation of adsorbed NH_3 into adsorbed N atoms readily occurs at 400°K and lower. Their conclusions were based mainly on two observations: (i) that the average work function changed from a value characteristic

of adsorbed NH_3 molecules to a value typical for adsorption of nitrogen on the tip, and (ii) the field emission pattern, which closely resembled that from adsorbed nitrogen, reverted to a clean pattern at about the same temperature that nitrogen desorbs. They had no mass spectrometer to identify the desorbing gases. On the basis of our present experiments and those of Estrup and Anderson,[18] we believe that these data of Dawson and Hansen are consistent with adsorbed NH_2 fragments rather than adsorbed N atoms.

In our present results, three different observations could have been misinterpreted by us were it not for the flashoff evidence of section I. Not only does the NH_2 "pseudo-N" structure decompose at about the same temperature as nitrogen desorption from W(211), but the LEED patterns of pure nitrogen and the "pseudo-N" are similar. In addition, the work function of an NH_2 covered surface is close to the clean surface value. Without flashoff information all these data could have been interpreted in terms of adsorbed N rather than NH_2. It is this somewhat fortuitous similarity between adsorbed NH_2 and adsorbed N that led Dawson and Hansen to their interpretation, an interpretation we feel needs changing in view of our LEED and flashoff results. Except for this basic difference of interpretation, their data show in many other respects a close correspondence with the present work and with that of Estrup and Anderson.[18]

It is important to have estimates of the magnitude of enthalpy changes as ammonia is degraded. We have listed in Table VI the enthalpies of several reactions. The enthalpies

ΔH_2, ΔH_5 and ΔH_6 refer to dilute coverage on evaporated W films rather than to a (211) face, and the numbers we shall calculate are therefore only approximately correct.

Our observation that adsorbed nitrogen and NH_2 groups (as "pseudo-N") have similar diffraction patterns, and are removed from the surface at about the same temperature, makes calculations of the bond energy D_1 for N atoms adsorbed dissociatively upon the surface and the bond energy D_2 for isolated NH_2 groups upon the surface especially interesting. We can write $D_1 = (1/2)\Delta H_1 + (1/2)\Delta H_2$ and $-D_2 + 2D_3 + (1/2)\Delta H_2 + \Delta H_3 + \Delta H_4 = 0$ where D_3 is the bond energy of N-H bonds. We obtain D_1 = 160 kcal/g atom and, assuming D_3 = 86 kcal/g atom which is the normal value for this bond,[56] D_2 = 156.5 kcal/g atom. The agreement is surprisingly good.

We can try to visualize in approximate fashion the thermochemical history of NH_3 molecules as they are decomposed by the surface. This is illustrated schematically in Fig. 27. Gas phase NH_3 molecules (ΔH_f = - 11 kcal/mole) are adsorbed at room temperature with heat of adsorption ΔH_5 = - 72 kcal/mole. Heating the surface to 500°K causes evaporation of hydrogen and formation of adsorbed NH_2 (with an estimated activation energy indicated in the figure). Heating to high temperatures causes decomposition of the adsorbed NH_2 by one of two postulated routes. Our present speculation is that the route indicated by the dashed line is followed during expansion of the C(4x2) structure until it is transformed into the "pseudo-N" structure.

Then the stepwise route of the solid line is followed as the "pseudo-N" structure is quite abruptly decomposed with evolution of molecular N_2 and atomic H. (NH radicals and adsorbed N atoms are assumed to be formed in rapid succession and with short lifetimes as intermediates). According to this the expanded structures derived directly from the C(4x2) represent always NH_2 radicals with evolution of very small amounts of H_2 and N_2 molecules as expansion occurs. The N_2 evolution in this region was not checked by the mass spectrometer, so it seems possible that during expansion the surface becomes slightly richer in nitrogen; this seems to us unlikely, however, largely because of the simplicity of the changing structures so readily accounted for by strictly stoichometric NH_2 radicals.

Our view that below 1050°K evaporation of hydrogen may be molecular rather than atomic is based on the following hypothesis. In the region of coverage of <u>reversible</u> expansion of NH_2 overlayers between C(4x2) and P(3x2), the surface seems ideally suited to act as intermediary in the decomposition of NH_3. That is to say, NH_3 molecules adsorbed on such expanded structures decompose to give NH_2 which can be taken up within the overlayer. At appropriate temperatures, NH_2 also decomposes within the layer with desorption of nitrogen and molecular hydrogen. For an equilibrium flow of ammonia, adsorption into the overlayer and desorption of nitrogen and hydrogen could be in balance. The reason for suggesting <u>molecular</u> hydrogen desorption in this range of coverage and temperature is to

explain how the same NH_2 surfaces could catalyze ammonia synthesis. The principle of microscopic reversibility demands that molecular hydrogen be adsorbed during synthesis and therefore desorbed during decomposition under these conditions.

At the present time it is too early to assess the new data presented here, and in related work,[16-18] in terms any stronger than at a level of hypothesis for the mechanism of ammonia decomposition on tungsten. The decomposition behavior is sensitive to the particular orientation of the surface, making generalization difficult. In fact, there is evidence that ammonia is not appreciably adsorbed on the W(110) surface[57] and therefore the (110) surface is probably inactive for both decomposition and synthesis of NH_3. There is not only sensitivity to orientation, but also the surface bonding is not simple for the single plane which we are studying here. Finally, we mention the NH_3 - D_2 exchange reaction which has been extensively studied. The mixing of desorbed low-temperature hydrogen in Peaks A_1 and A_2 (Fig. 6) is related to this problem, as indicated by the research of Kemball.[47] Work is required upon the NH_3 - D_2 exchange using single crystal tungsten surfaces.

We have seen that ammonia decomposes on a tungsten (211) surface in two main stages. The first stage gives adsorbed NH_2 radicals which are thermally destroyed in a second stage at elevated temperatures with evolution of both nitrogen and hydrogen. Nitrogen is never evolved unaccompanied by hydrogen (see also Estrup and Anderson[18]). Tamaru's conclusion[12] that nitrogen desorption is rate controlling is apparently in conflict with

the experimental fact[7,8] that ND_3 decomposes more slowly than NH_3. We now see there is no difficulty of interpretation, because thermal decomposition of adsorbed NH_2 takes place at the same temperature as evaporation of adsorbed nitrogen.

REFERENCES

1. C. N. Hinshelwood and R. E. Burk, J. Chem. Soc. 127, 1105 (1925).
2. G. M. Schwab, Z. Physik. Chem. 128, 161 (1927).
3. C. H. Kunsman, J. Amer. Chem. Soc. 50, 2100 (1928).
4. C. H. Kunsman, E. S. Lamar and W. E. Deming, Phil. Mag. 10, 1015 (1930).
5. H. R. Hailes, Trans. Faraday Soc. 27, 601 (1931).
6. W. Frankenburger and A. Hodler, Trans. Faraday Soc. 28, 229 (1932).
7. J. C. Jungers and H. S. Taylor, J. Amer. Chem. Soc. 57, 679 (1935).
8. R. M. Barrer, Trans. Faraday Soc. 32, 490 (1936).
9. N. Nagasko and S. Miyazaki, Bull. Tokyo Inst. Technology 13, 124 (1948); (Chem. Abst. 44, 10552 (1950).
10. M. Wahba and C. Kemball, Trans. Faraday Soc. 49, 1351 (1953).
11. S. R. Logan and C. Kemball, Trans. Faraday Soc. 56, 144 (1960).
12. K. Tamaru, Trans. Faraday Soc. 57, 1410 (1961).
13. Review articles are in "Catalysis" (P. H. Emmett, ed.), Reinhold, New York, 1954; G. C. Bond, "Catalysis by Metals" p 371, Academic Press, New York 1962; K. Tamaru, Adv. Catalysis 15, 65 (1964).
14. K. Azuma, Nature 190, 530 (1961).
15. K. Azuma, J. Res. Inst. Catalysis Hokkaido Univ. 9, 55 (1961).
16. P. T. Dawson and R. S. Hansen, J. Chem. Phys. 45, 3148 (1966); 48, 623 (1968).

17. J. Anderson and P. J. Estrup, Surface Sci. 9, 463 (1968).

18. P. J. Estrup and J. Anderson, J. Chem. Phys. (1968). in press.

19. F. W. Lampe, J. L. Franklin and F. H. Field, J. Amer. Chem. Soc. 79, 6129 (1957).

20. A. J. B. Robertson and E. M. A. Willhoft, Trans. Faraday Soc. 63, 476 (1967).

21. Mass Spectral Data, Vol. I, Serial Number 90 Amer. Petroleum Res. Inst. Project 44, Chem. Thermo. Properties Center, A and M College of Texas, College Station, Texas.

22. R. A. Armstrong, Can. J. Phys. 44, 1753 (1966).

23. P. A. Redhead, Vacuum 12, 203 (1962).

24. T. W. Hickmott, J. Chem. Phys. 32, 810 (1960).

25. P. A. Redhead, Proc. Symposium on Electron and Vacuum Physics, Hungary (1962) p. 89.

26. V. J. Mineault and R. S. Hansen, J. Chem. Phys. 45, 2240 (1966).

27. W. J. M. Rootsaert, L. J. van Reijen and W. M. H. Sachtler, J. Catalysis 1, 416 (1962).

28. C. C. Chang, Ph. D. Thesis, Cornell University (1967).

29. L. J. Rigby, Can. J. Physics 43, 1020 (1965).

30. O. Beeck, Adv. Catalysis 2, 151 (1950) - see Fig. 2 of this reference.

31. E. Molinari, F. Cramarossa, M. Capitelli and A. Mercanti, Ricerca Sci. 36, 109 (1966).

32. C. E. Melton and P. H. Emmett, J. Phys. Chem. 68, 3318 (1964).

33. D. Brennan and P. C. Fletcher, Proc. Roy. Soc. A250, 389 (1959).

34. E. Bauer, Surface Science 7, 351 (1967).

35. N. H. Fletcher, J. Appl. Phys. 35, 234, 22 76 (1964).

36. G. C. Pimentel and A. L. McClellan "The Hydrogen Bond" Freeman and Co., San Francisco (1960) p. 262.

37. D. A. Ramsay, J. Chem. Phys. 25, 188 (1956).

38. J. R. Sabin, Intl. J. Quantum Chem. 2, 23 (1968).

39. J. R. Sabin, private communication.

40. R. L. Gerlach and T. N. Rhodin, Surface Sci. 10, 446 (1968).

41. P. W. Palmberg and T. N. Rhodin, in press, J. Chem. Phys. June (1968).

42. The authors are much indebted to J. C. Tracy, Jr., for his valuable help in carrying out the work function measurements. Details of the apparatus are described in J. C. Tracy, Jr., Ph. D. Thesis, Cornell University (1968) - in preparation.

43. A. A. Holscher, Dissertation, Leiden University, Netherlands (1967) p 63.

44. U. Feldman and M. Folman, Trans. Faraday Soc. 60 440 (1964).

45. J. Weber and J. K. Laidler, J. Chem. Phys. 19, 381, 1089 (1951).

46. J. H. Singleton, E. R. Roberts and E. R. S. Winter, Trans. Faraday Soc. 47, 1318 (1951).

47. C. Kemball, Proc. Roy. Soc. A214, 413 (1952).

48. A. Ozaki, H. Taylor and M. Boudart, Proc. Roy. Soc. A258, 47 (1960).

49. P. M. Gundry, J. Haber and F. C. Tompkins, J. Catalyis 1, 363 (1962).

50. K. Tamaru, K. Tanaka, S. Fukasaku and S. Ishida, Trans. Faraday Soc. 61, 765 (1965).

51. T. Nakata and S. Matsushita, J. Phys. Chem. 72, 458 (1968).

52. O. Beeck, Adv. Catalysis 2, 151 (1950).

53. M. Scwarc, Chem. Rev. 47, 75 (1950).

54. J. A. Kerr, R. C, Sekhar and A. F. Trotman - Dickenson, J. Chem. Soc. (1963) 3217.

55. J. A. Kerr, A. F. Trotman - Dickenson and M. Wolter, J. Chem. Soc. (1964) 3584.

56. Handbook of Chemistry and Physics, 44th Edition, The Chemical Rubber Publishing Co., Cleveland (1962) p. 3519.

57. J. W. May, unpublished results.

TABLE I

Surface Coverage and Composition

	10^{15} Molecules in Peak B				$\frac{\text{B hydrogen}}{\Sigma A_1 \text{ hydrogen}}$	$\frac{\text{B hydrogen}}{\text{B nitrogen}}$
	Hydrogen Molecules		Nitrogen Molecules			
	Flash-off Value (Fig. 8)	Calculated from LEED Pattern (Sec. II)	Flash-off Value (Fig. 9)	Calculated from LEED Pattern (Sec. II)	(Fig. 8)	(Figs.8,9)
One Dose	1.4	---	0.66	---	1.9	2.1
Three Doses	2.1	1.84	1.0	0.92	2.0	2.1

TABLE II

Four Simple Overlayer Structures

Pattern	α	NH_2 Coverage (Θ)*	Overlayer Unit Mesh Dimension in $[1\bar{1}1]$, A	Overlayer Mesh Dimension in $[01\bar{1}]$, A	Area per NH_2 (A^2)
C(4x2)	0.750	2.25	3.65	2.98	5.43
P (7x2)	0.714	2.14	3.83	2.98	5.70
C(10x2)	0.700	2.10	3.91	2.98	5.82
P(3x2)	0.667	2.00	4.10	2.98	6.11

* 1 monolayer = number of W atoms in a (211) plane = $(2/3)^{1/2} a_o^{-2} = 8.19 \times 10^{15}$ cm^{-2}.

TABLE III

Structural Characteristics of NH_2 Overlayers

Structure	N...H...N Distance (A)	Obtuse Angle HNH (deg.)
C(4x2)	2.35	101.4
P(7x2)	2.42	104.2
C(10x2)	2.46	105.4
P(3x2)	2.53	108.1

TABLE IV

Simplest Double Scattering Combinations for the Index h of Some Beams of the C(10x2) Pattern*

h	m = m'	Structure of Fig. 21 p	Structure of Fig. 22 p' = p - m
1/10	3	-2	-5
2/10	-4	3	7
3/10	-1	1	2
4/10	2	-1	-3
5/10	5	-3	-8
6/10	-2	2	4
7/10	1	0	-1
8/10	4	-2	-6
9/10	-3	3	6

* $h = p + \alpha m = p' + (1 + \alpha)m'$ and $\alpha = 7/10$

TABLE V

Work Function Changes on W(211)

Adsorbate	$\Delta\phi$ (eV)	Reference
NH_3	-0.8	This paper
NH_2	0.0	This paper
NH_3 upon NH_2	-0.9	This paper
H_2	+0.65	22
N_2	+0.43	43

TABLE VI

Enthalpy Changes

Reaction	Description	Enthalpy Change kcal	Reference
$N_2 \rightarrow 2N_{gas}$	$\Delta H_1 = D(N\text{-}N)$	+225	
$2N_{ads} \rightarrow N_2$	ΔH_2= Heat of desorption from evaporated W film	+ 95	52
$2H_{gas} \rightarrow H_2$	$\Delta H_3 = -D(H\text{-}H)$	-103	
$\frac{1}{2}N_2 + H_2 \rightarrow (NH_2)_{gas}$	$\Delta H_4 = \Delta H_f(NH_2)_{gas}$	+ 40	53-55
$NH_3 \rightarrow (NH_3)_{ads}$	ΔH_5=Heat of adsorption on evaporated W film	- 72	10
$H_2 \rightarrow 2H_{ads}$	ΔH_6=Heat of adsorption on evaporated W film	-45	52

FIGURE CAPTIONS

Figure 1. Typical mass spectrum after $N^{15}H_3$ ahd been flowing through Vacion-pumped apparatus for several days. Gas mixture: H_2 - 2.5×10^{-7}, $N^{15}H_3$ - 1.6×10^{-7}, $^{30}N_2$-0.4×10^{-7} torr. Note high partial pressure of H_2 after this long flow. Peaks at 16, 17 and 18 are cracking pattern of ammonia. Peaks at 15, 28, 29 and 30 are atomic and molecular nitrogen from decomposed ammonia. Partial pressure of CO < 5×10^{-10} torr.

Figure 2. Hydrogen was first adsorbed at room temperature for 12, 60 and 240 sec at 5×10^{-8} torr (exposures of 0.6, 3 and 12 L). Heating rate during desorption about 60° sec^{-1}.

Figure 3. Development of α plus β and γ peaks as function of hydrogen exposure (see Fig. 2).

Figure 4. Hydrogen evolution after coadsorption of ammonia and hydrogen. NH_3 pressure 1.0×10^{-8} torr, H_2 pressure 1.7×10^{-8} torr. Exposure time 350 sec. Peaks A_1 and B are characteristic of ammonia, peak A_2 comes from hydrogen adsorbed directly (see γ peak of Fig. 2). Initial heating rate 200° sec^{-1}.

Figure 5. Room temperature displacement of hydrogen by ammonia. Hydrogen desorption traces after ammonia exposures of 3, 6 and 12 L with $P_{NH_3} = 1.0 \times 10^{-8}$ and $P_{H_2} = 0.7 \times 10^{-7}$ torr. Initial heating rate 150° sec^{-1}. Figure illustrates decrease of peak A_2 and growth of peak A_1 with increasing

exposure to the ammonia-hydrogen mixture. (Peak B, not shown - see Fig. 4, grows also with exposure.)

Figure 6. Flash-off results after NH_3 exposures of 3.5 L for different amounts of added hydrogen. Peak A_2 is not found for high ratios of ammonia to hydrogen. Note the constant hydrogen/nitrogen ratio of peak B appropriate to NH_2.

Figure 7. Fraction of hydrogen flashed off in peak A_1 that is not from NH_3, plotted against experimental values of peak B hydrogen. Data from Fig. 6. When this fraction falls to zero the value of peak B is 1.3×10^{15} molecules cm^{-2} which corresponds to a sticking probability of NH_3 of 0.8 in the absence of hydrogen.

Figure 8. Hydrogen flashed off after a single saturating exposure to NH_3 (90 L) - curves marked (1); and after further saturating exposures with intermediate flashing to 800°K to remove the A_1 hydrogen, (2) and (3).

Figure 9. Same as Fig. 8 - for nitrogen.

Figure 10. Desorption from surface having a saturated NH_2 layer. Superposed traces for nitrogen and hydrogen evolution are shown below (initial heating rate 200° sec^{-1}). Integrated amounts of hydrogen and nitrogen reaching the mass spectrometer are shown above.

Figure 11. (a) Fully-saturated NH_2 surface flashed successively to higher and higher experimental temperatures above 800°K (direction of arrows). Ammonia readsorbed

between flashes. Temperature at wich B hydrogen peak begins to desorb is plotted against these experimental temperatures. (b) Temperature of the maximum of B hydrogen peak for various fractions of complete NH_2 coverage.

Figure 12. Model of bcc (211) surface showing orientation for all LEED patterns. Figure shows positioning of crystal with respect to beam. The [211] direction is pointing toward the electron gun. Dimensions of unit mesh (outlined) are $(3^{\frac{1}{2}}/2)a_o x 2^{\frac{1}{2}}a_o$ with a_o = 3.16Å for tungsten. All diffraction patterns are referred to this orientation of the crystal.

Figure 13. LEED patterns at normal incidence, from clean W(211) at top, hydrogen-covered (middle) and ammonia-covered (bottom). Left and right hand columns, respectively 55 and 90 eV. Illumination of crystal supports is by mass spectrometer filament (in the hydrogen patterns).

Figure 14. Patterns at 90 eV after saturation room temperature exposures to NH_3 followed by heating. A, B, C: each one dose and one heating, respectively to 750, 800 and 850°K. D and E: respectively two doses and three doses, heated to 875°K after each dose. Patterns observed at room temperature. Sequence A, B, C shows development of an ordered C(4x2)-NH_2 structure, with degree of order dependent on flashing temperature. The photos of D and E illustrate intensification of

the LEED patterns after redosing, and show also that relative intensities of extra spots are not significantly affected by redosing. Light from mass spectrometer filament is illuminating the crystal supports (A to D) but not in E (filament off).

Figure 15. Diffraction patterns at 90 eV from ammonia saturated surface heated to 1000°K. Symmetry is C(10x2). (a) one dose (b) three doses.

Figure 16. LEED patterns at 90 eV from a surface first saturated with NH_2 by redosing, and then heated above 900°K. The sequence A to H were obtained after heating to progressively higher temperatures, as tabulated below.

	Max. Temp. °K	α	Calculated NH_2 coverage (monolayers)
A	910	0.738	2.21
B	920	0.727	2.18
C	935	0.719	2.16
D	955	0.714	2.14
E	970	0.707	2.12
F	1000	0.700	2.10
G	1030	0.687	2.06
H	1040	0.675	2.03

Patterns of D and F are respectively P(7x2) and C(10x2).

Figure 17. Schematic diagram of C(4x2) pattern (compare with Fig. 14e). Filled circles represent primary beams from the

substrate, and crosses-in-circles primary beams of a centered NH_2 overlayer. One of these overlayer beams is indexed $\overline{3/4}\ \overline{3/2}$ referred to the substrate; it is the $\bar{1}\bar{1}$ beam of the overlayer. Multiple scattering between overlayer and substrategives rise to all the other reflections (light crosses).

Figure 18. Sketches of the simplest composite structures, showing their unit meshes. Open circles represent NH_2; filled circles, top layer W atoms of substrate. Structures are arranged in order of increasing unit edge of the overlayer mesh from 3.65Å to 4.10Å.

Figure 19. Expansion of NH_2 overlayers in the temperature range 900 - 1050°K. For each experimental point the surface was first saturated with NH_2 by repeated dosing, then flashed to the temperature of the abscissa. Values of α were computed from measurements of the LEED pattern obtained after cooling. Crosses and circles represent values of α deduced from sets of measurements of two types. The photos of Fig. 16 were used (and others). Three different scales of ordinates are marked on the figure; at left - α; at right - coverage Θ and unit mesh edge of overlayer parallel to the troughs of the substrate (in Angstrom units).

Figure 20. Measurements of amounts of H_2 flashed off in the temperature range 900 to 1050°K, each point representing a separate experiment starting with a single saturation

room temperature dose of NH_3. The amounts are given as fractions of the total amount of H_2 in the C(4x2) structure after one dose. Temperatures at which P(7x2) and C(10x2) are found are marked by arrows. The theoretical fraction 0.11 for formation of P(3x2) is marked also. At about this point the surface arrangement is drastically changed into what we call the "pseudo-N" structure.

Figure 21. Proposed model of the C(4x2)-NH_2 structure. The centers of substrate W atoms are shown as black dots. The overlayer atoms are drawn to scale as open circles (N diameter = 1.50Å, H diameter = 0.74Å). A C(4x2) combination mesh is outlined and dimensions within the overlayer are also shown. A plausible placing of the overlayer is given (differing from others only by translations of the overlayer parallel to the surface). Within the overlayer H atoms are shared by N atoms with bonding analogous to hydrogen bonding. The N atoms are bonded to the substrate tungsten.

Figure 22. Model of C(4x2) not favored but discussed in text. Large circles are substrate W atoms, small circles NH_2 groups (hydrogen atoms not shown).

Figure 23. LEED patterns at 90 eV. (A) transition pattern with incipient "pseudo-N" pattern. Note presence of beams attributable to P(3x2), and high background indicating a disordered surface structure (crystal supports illuminated by mass spectrometer filament). (B) "Pseudo-N" pattern.

Figure 24. LEED patterns at 90 eV. (A) Pattern from P(7x2) structure without second layer physisorbed NH_3 molecules (B) After exposure to NH_3. Disordered second layer of NH_3 molecules gives rise to high background and suppression of multiple scattering beams involving high orders. Beams involving only low orders are still present.

Figure 25. Changes in work function with crystal exposed at room temperature to a gas mixture containing ammonia, hydrogen and nitrogen at respective partial pressures 3, 2 and $1x10^{-8}$ torr. Curve 1 Obtained after cleaning crystal by flashing to 1450°K for 1 sec. Ammonia displaces coadsorbed hydrogen, and nitrogen is not adsorbed (see Section I). Large decrease in work function is due to NH_3 molecules adsorbed without dissociation on the bare surface. Curve 2 Crystal next flashed once to 720°K to create NH_2 layer on surface plus extra sites. The newly adsorbed NH_3 lies in part upon first layer NH_2 and in part upon clean surface. Curve 3 Second layer adsorption of NH_3 upon a nearly complete NH_2 monolayer. Extrapolations of curves 2 and 3 show that $\Delta\phi$ for NH_2 covered surface is approximately 0.0 eV.

Figure 26. Continuation of the experiment of Fig. 25 which shows the first three flashes. The temperature of each flash is given below.

Flash No.	Temp. °K	Flash No.	Temp. °K
1	1450	12	400
2	720	13	490
3	750	14	560
4	750	15	610
5	720	16	670
6	760	17	720
7	720	18	780
8	760	19	850
9	760	20	760
10	330	21	1130
11	370	22	1450

$\Delta\phi$ for NH_2-covered surface without second layer NH_3 is $\sim$ 0.0 eV (see Fig. 25). Flashes 4-9 show the change in ϕ caused by a second layer of NH_3 upon a saturated primary layer of NH_2. The level for NH_3 upon a full layer of NH_2 ($\Delta\phi$ = -0.9 eV) is lower than after flash No. 2, possibly because of depolarization within the second layer. The same effect is seen when the NH_2 layer is partially removed (Flash 21). Flashes 10-13 demonstrate that second layer NH_3 molecules are thermally desorbed very readily.

Figure 27. Thermochemical history of ammonia decomposition on tungsten. It is assumed that below 1050°K decomposition follows the lower route to give molecular H_2, but above this temperature it follows the upper route to give atomic H.

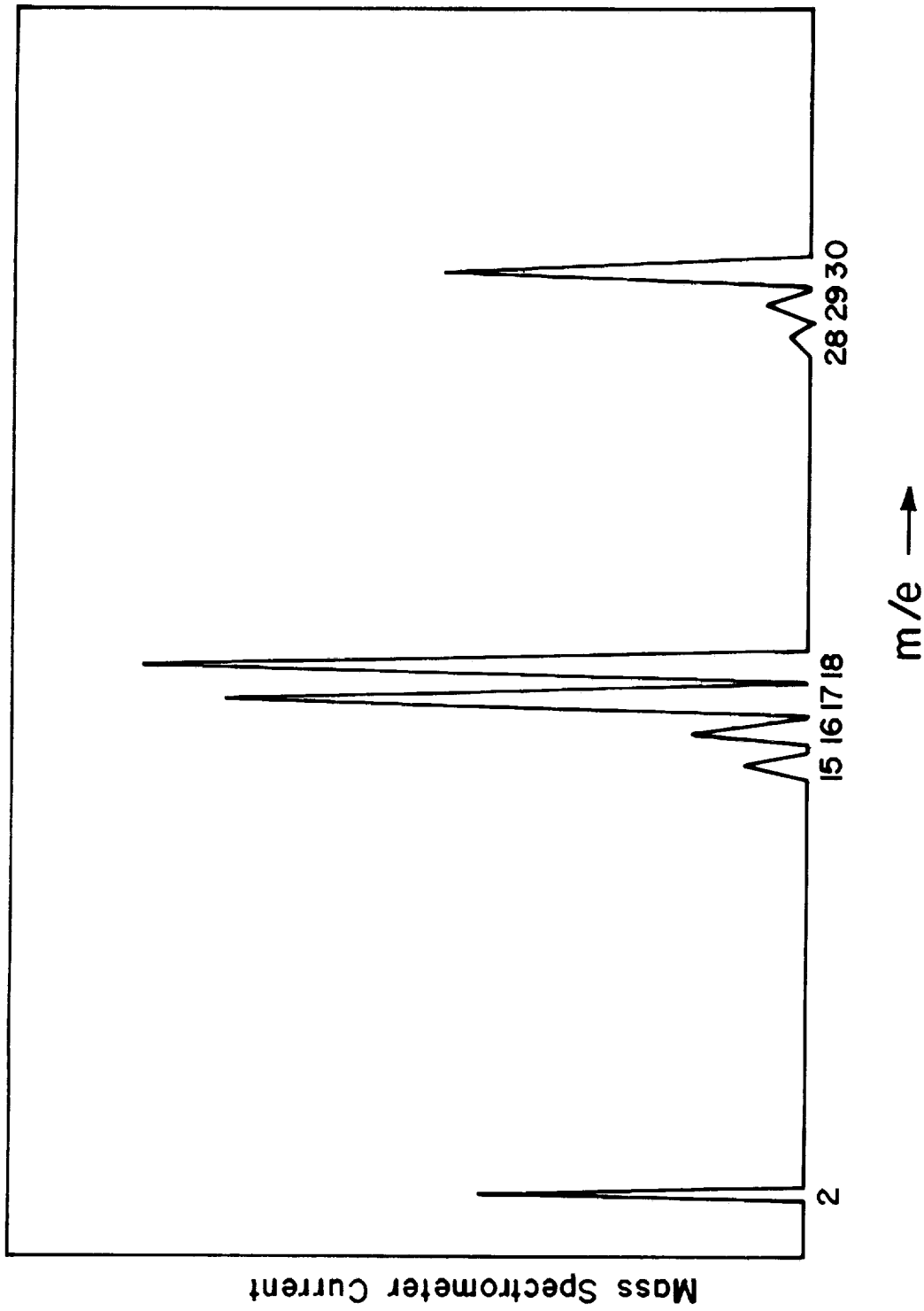

Figure 1

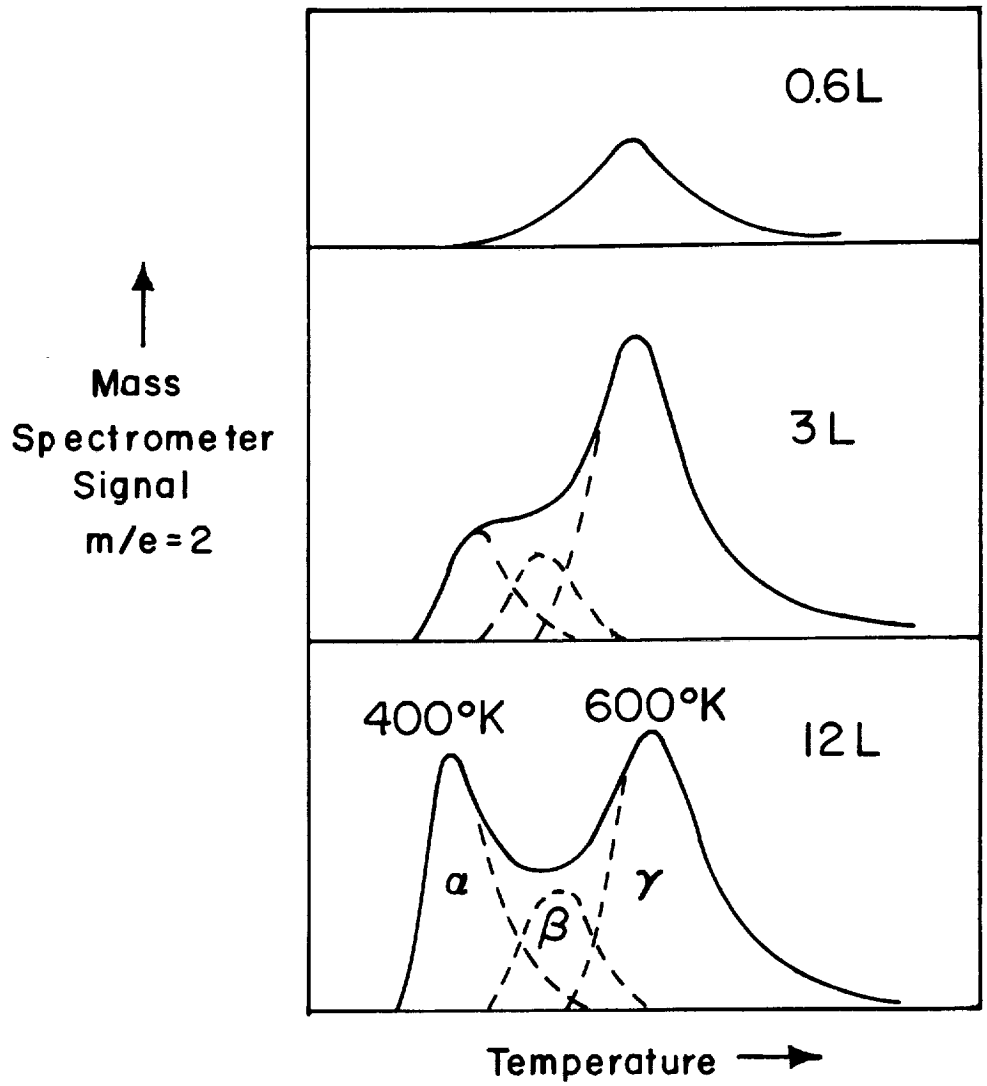
0.6L
3L
12L
400°K
600°K
α
β
γ
Mass
Spectrometer
Signal
m/e=2
Temperature

Figure 2

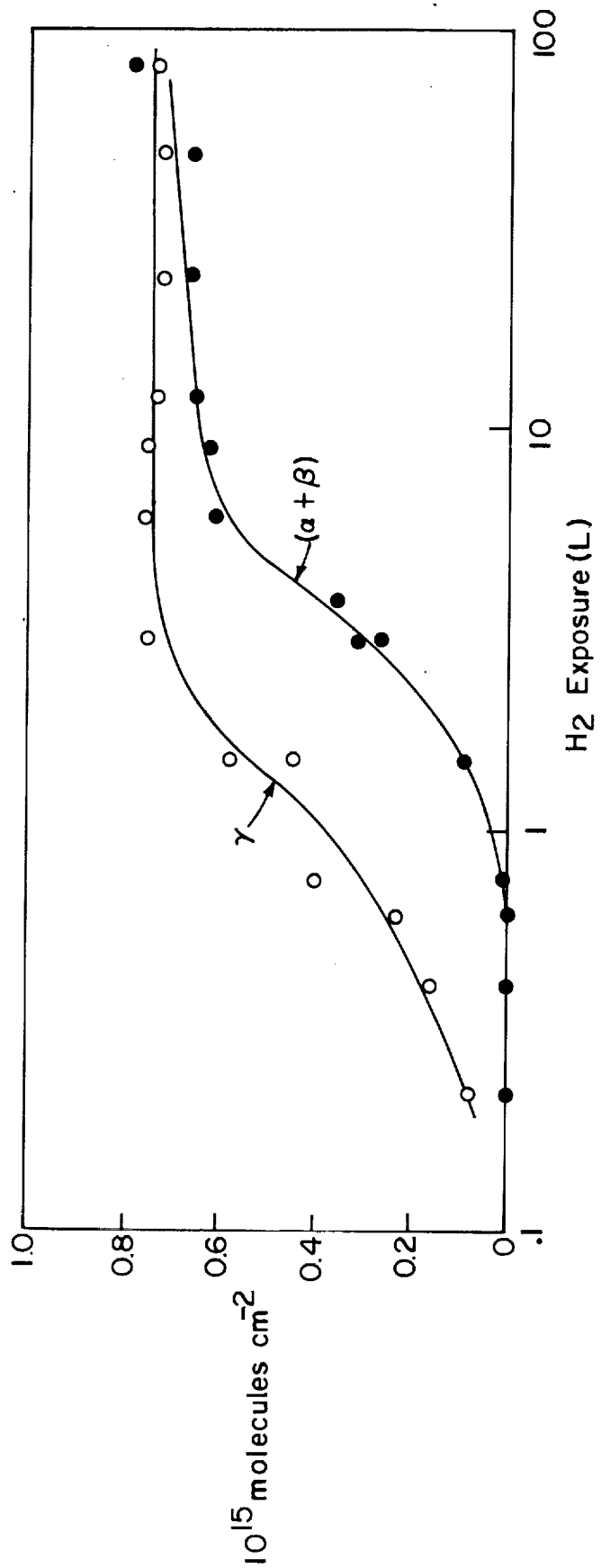

Figure 3

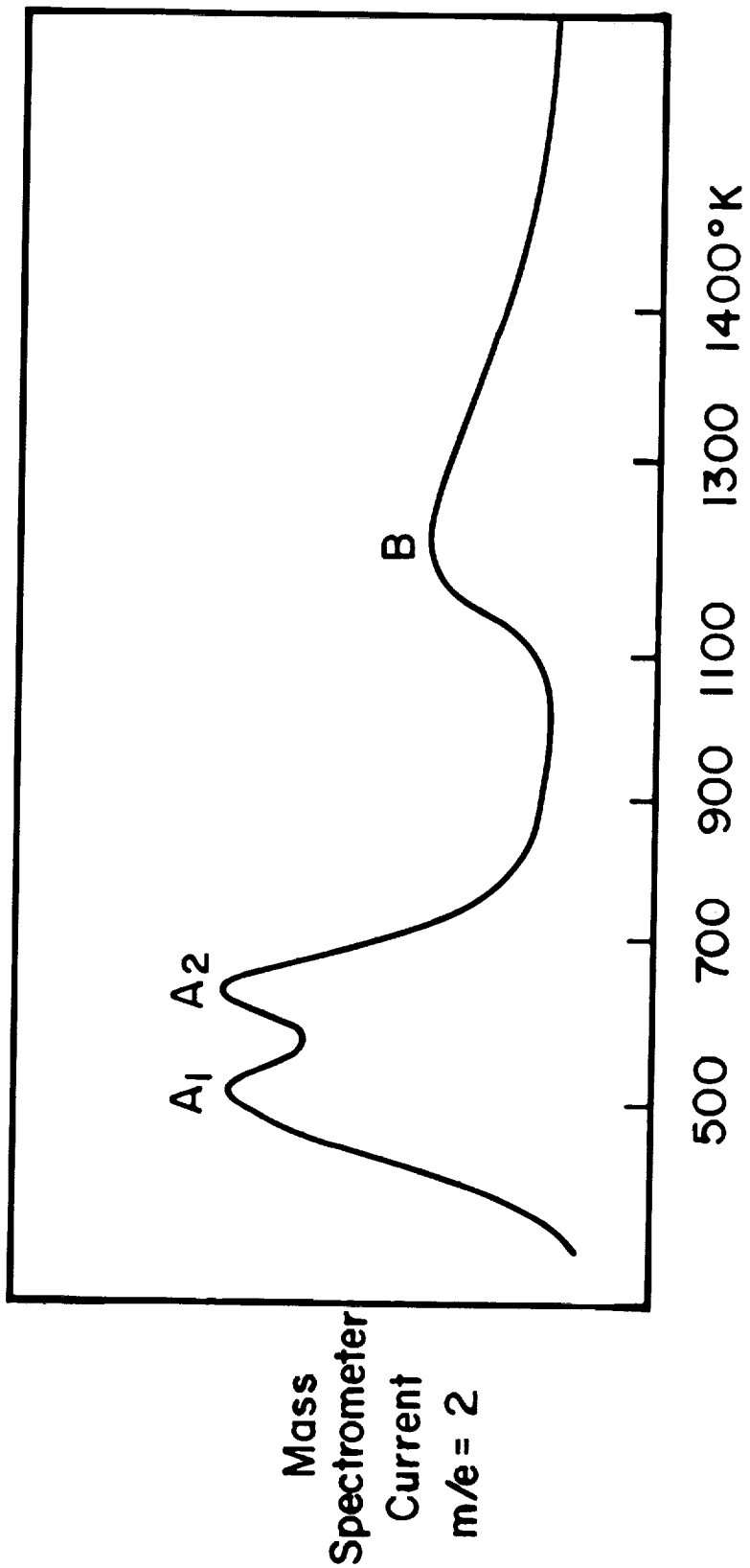
Mass
Spectrometer
Current
m/e = 2
A1
A2
B
500
700
900
1100
1300
1400°K

Figure 4

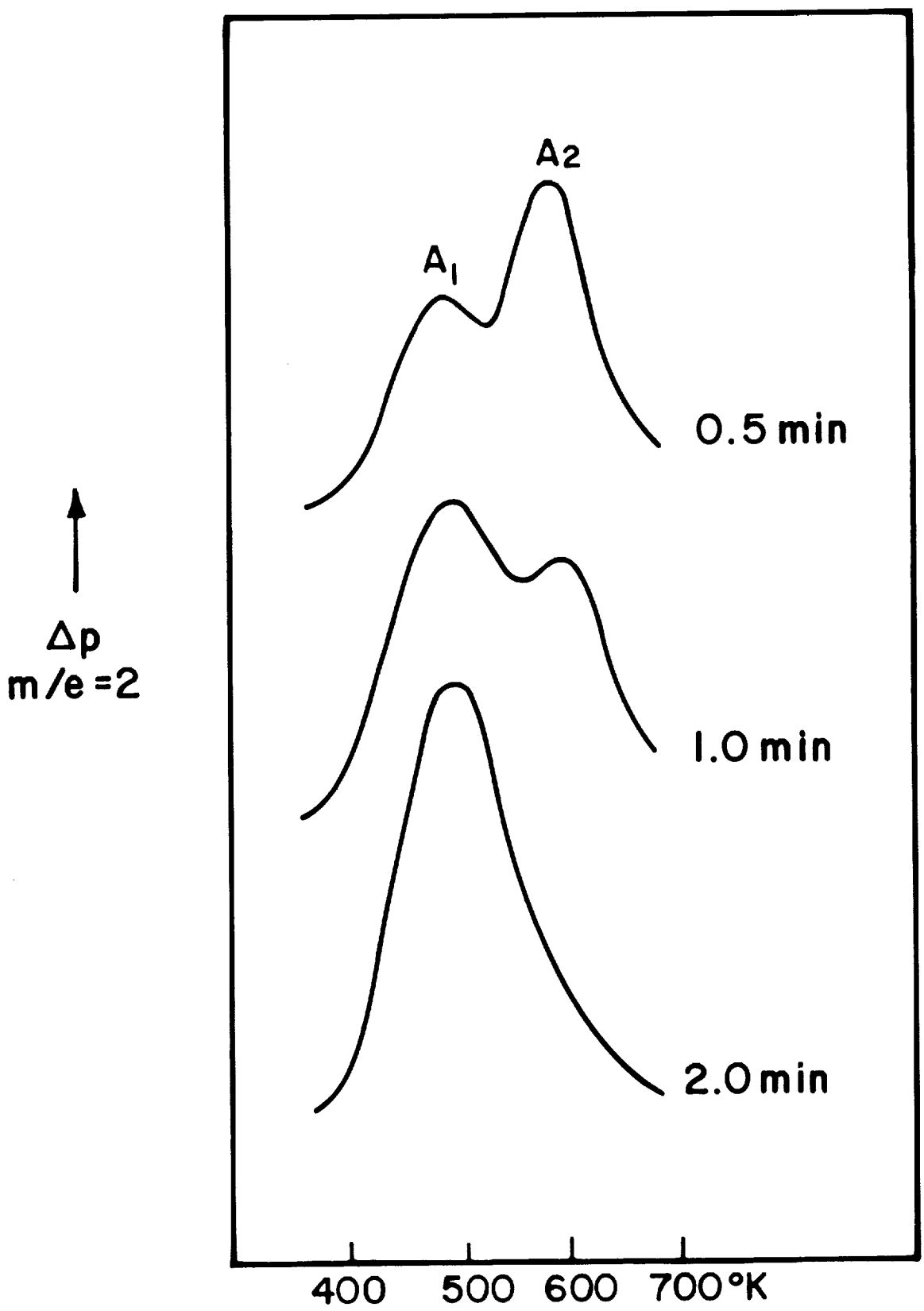

Figure 5

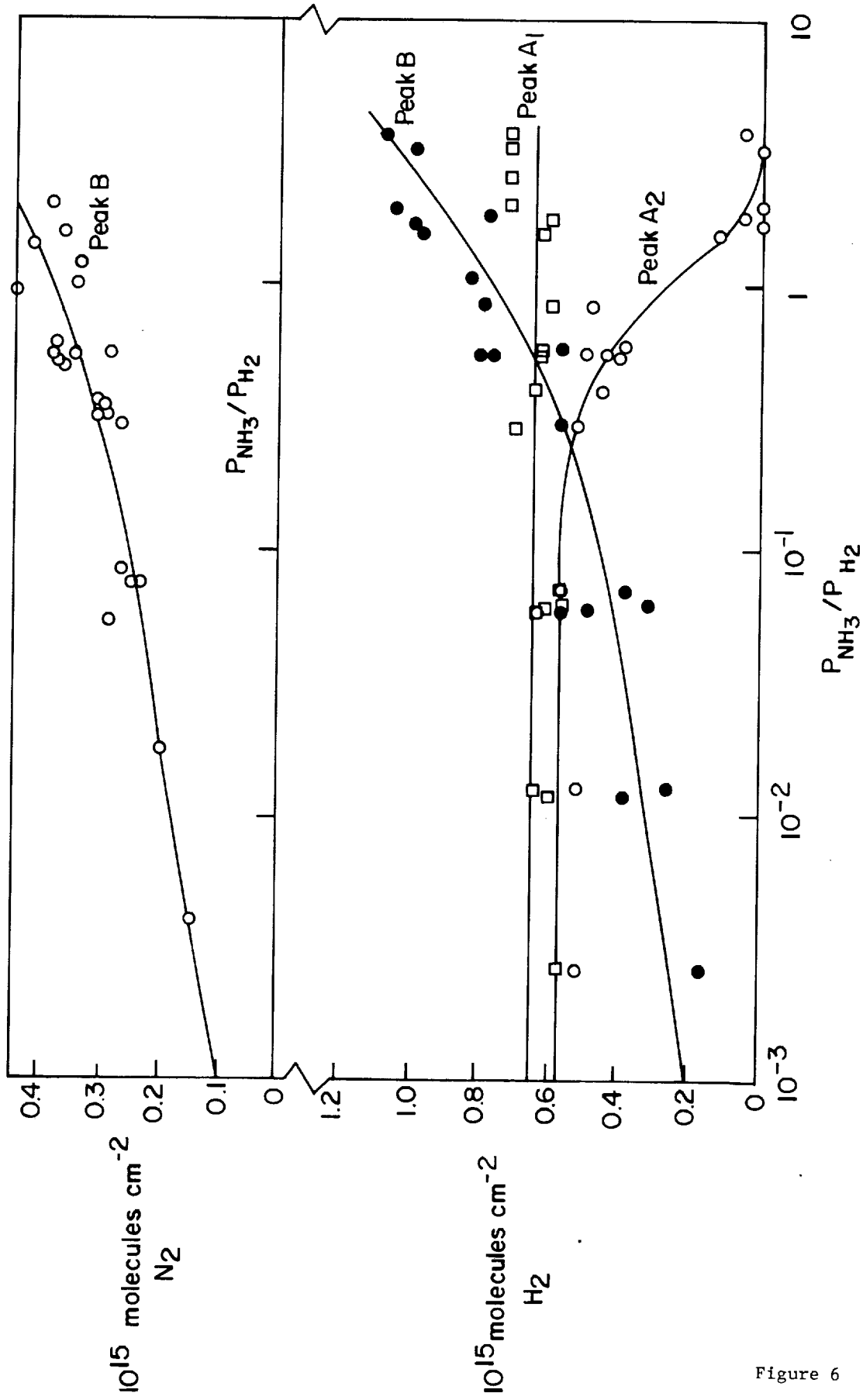
Peak B
Peak B
Peak A1
Peak A2
P_{NH_3}/P_{H_2}
P_{NH_3}/P_{H_2}
10^{15} molecules cm^{-2} N_2
10^{15} molecules cm^{-2} H_2
0.4
0.3
0.2
0.1
0
1.2
1.0
0.8
0.6
0.4
0.2
0
10
1
10^{-1}
10^{-2}
10^{-3}

Figure 6

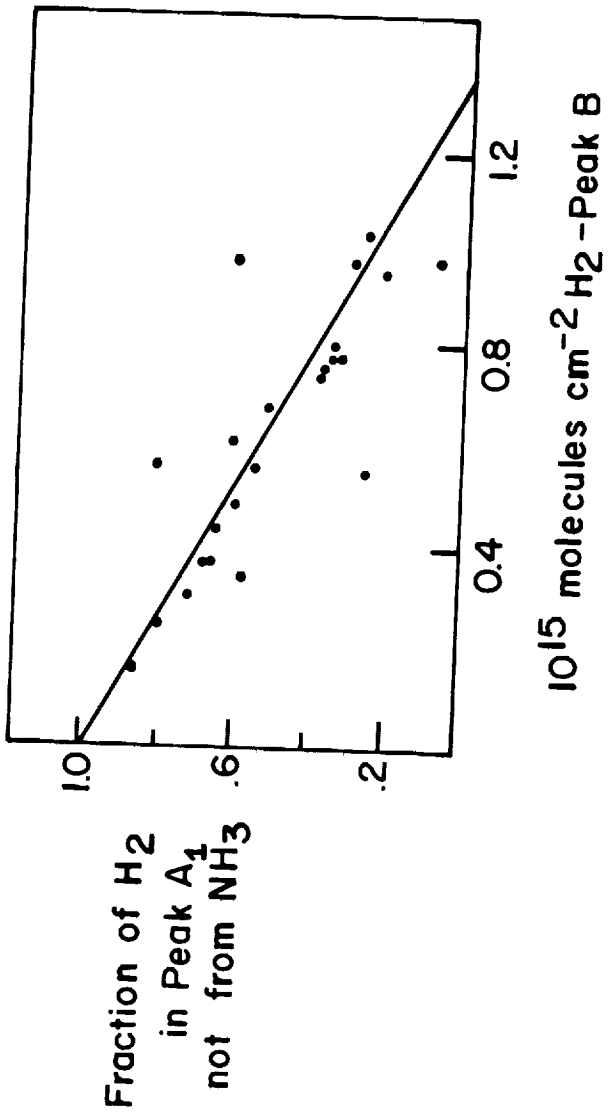
1.0
.6
.2
0.4
0.8
1.2
Fraction of H_2 in Peak A_1 not from NH_3
10^{15} molecules cm^{-2} H_2-Peak B

Figure 7

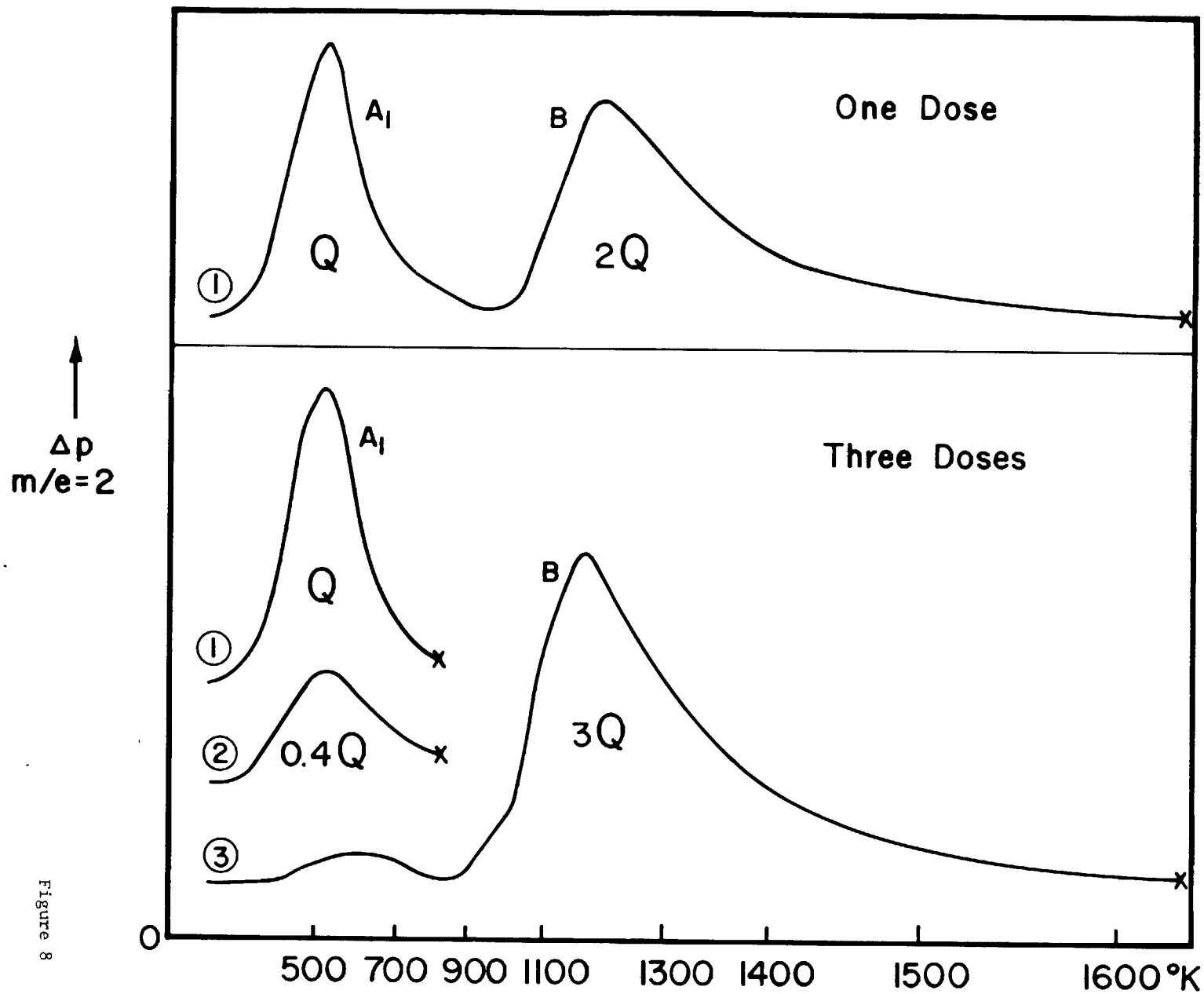
One Dose
A1
B
Q
2Q
①
Three Doses
A1
B
Q
①
②
0.4Q
3Q
③
Δp
m/e=2
0
500 700 900 1100 1300 1400 1500 1600°K

Figure 8

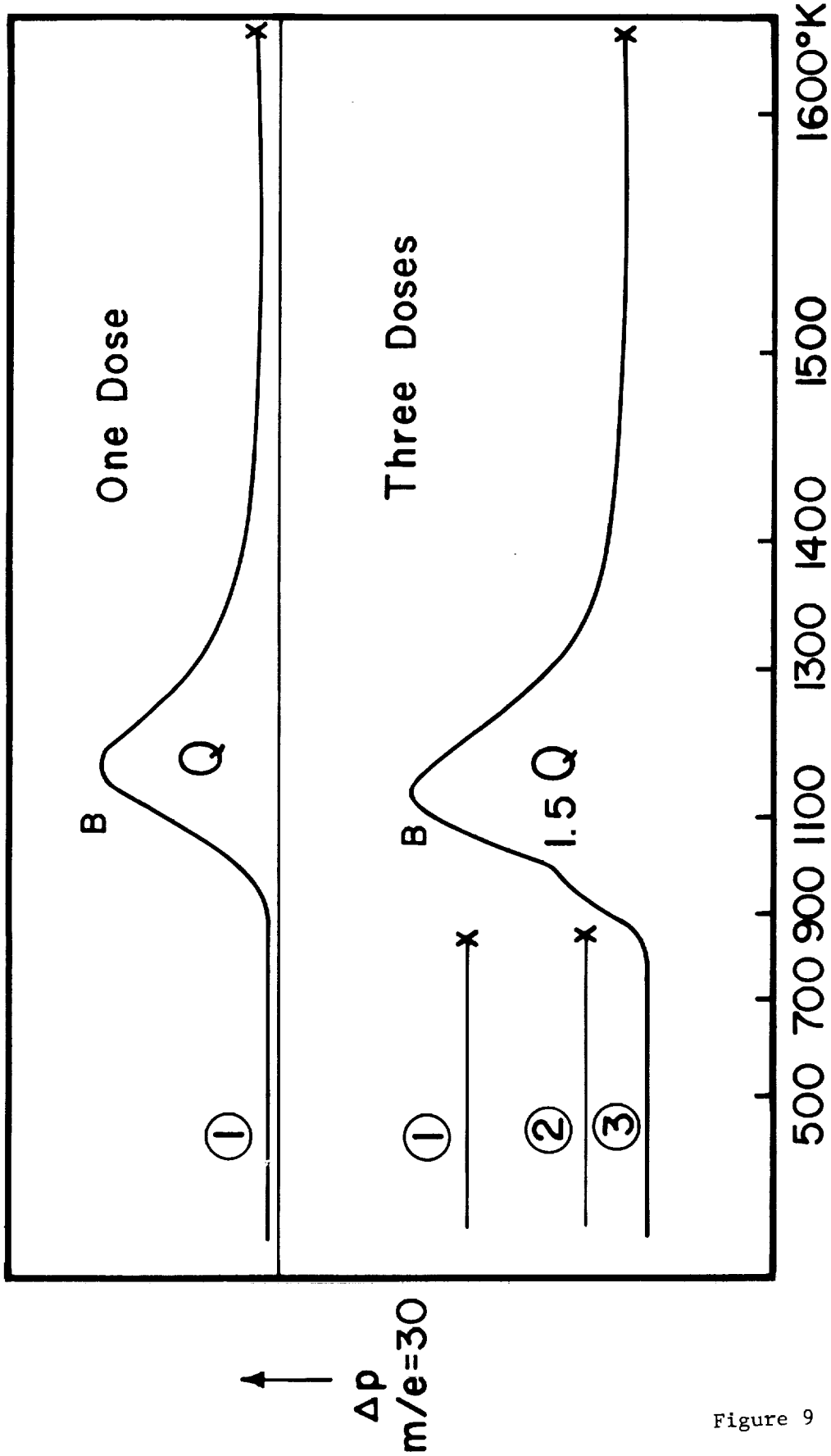
One Dose
Three Doses
B
Q
B
1.5 Q
①
①
②
③
500 700 900 1100 1300 1400 1500 1600°K
Δp
m/e=30

Figure 9

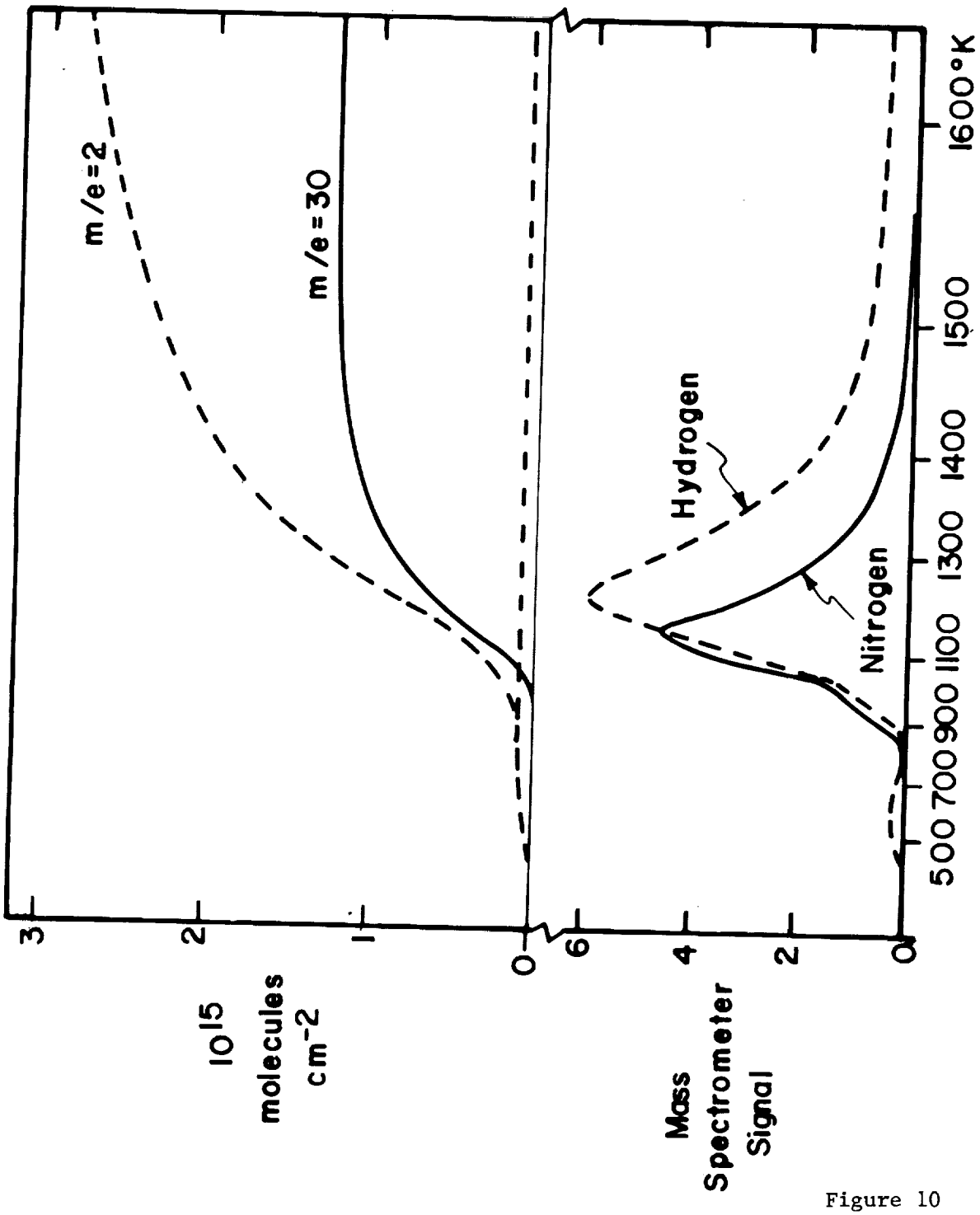
m/e=2
m/e=30
Hydrogen
Nitrogen
10^{15} molecules cm^{-2}
Mass Spectrometer Signal
500 700 900 1100 1300 1400 1500 1600°K
3 2 1 0
6 4 2 0

Figure 10

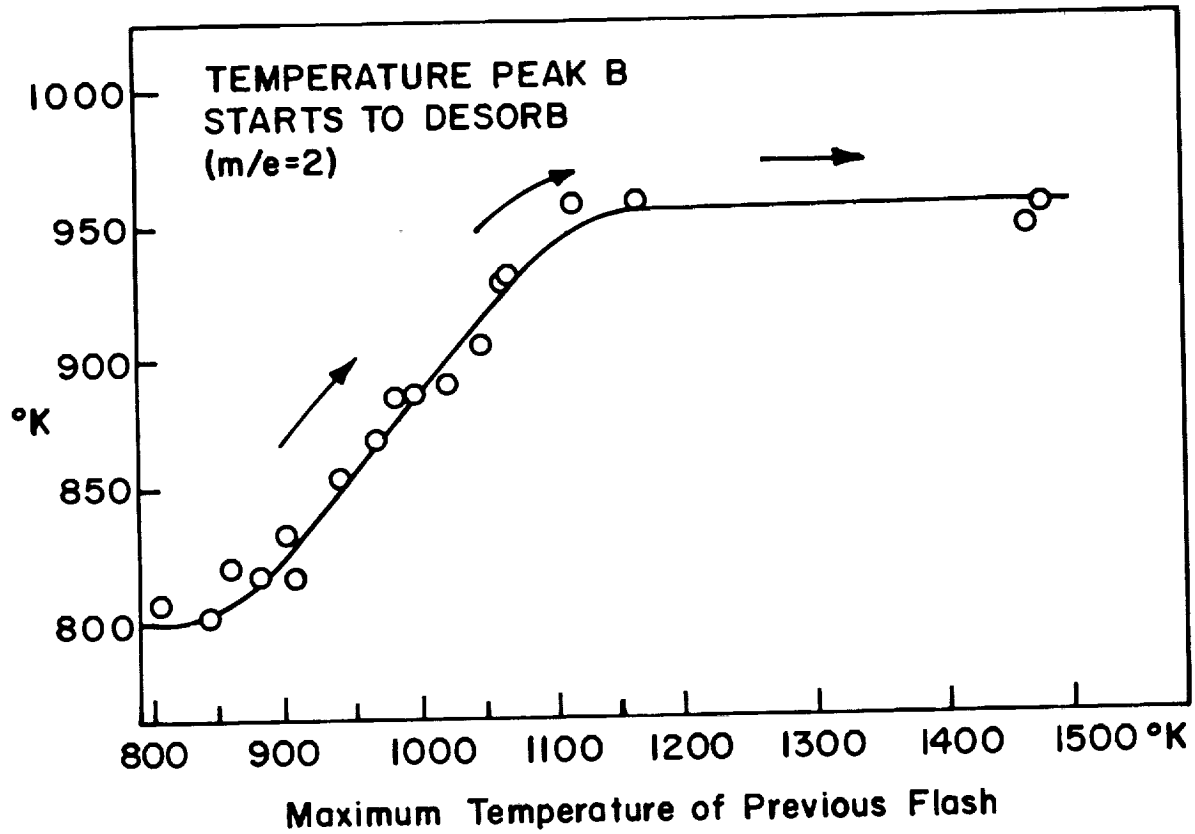
TEMPERATURE PEAK B
STARTS TO DESORB
(m/e=2)
1000
950
900
850
800
°K
800
900
1000
1100
1200
1300
1400
1500 °K
Maximum Temperature of Previous Flash

(a)

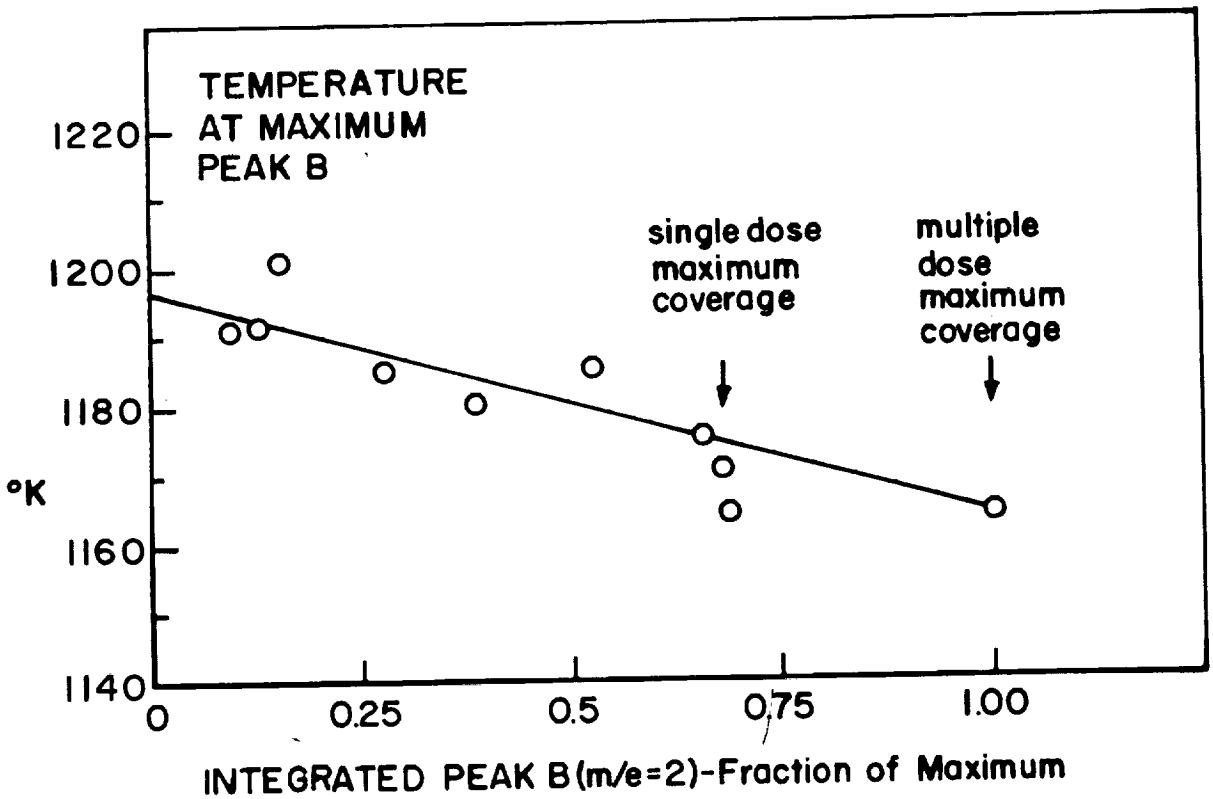
TEMPERATURE
AT MAXIMUM
PEAK B
single dose
maximum
coverage
multiple
dose
maximum
coverage
1220
1200
1180
1160
1140
°K
0
0.25
0.5
0.75
1.00
INTEGRATED PEAK B(m/e=2)-Fraction of Maximum

(b)

Figure 11

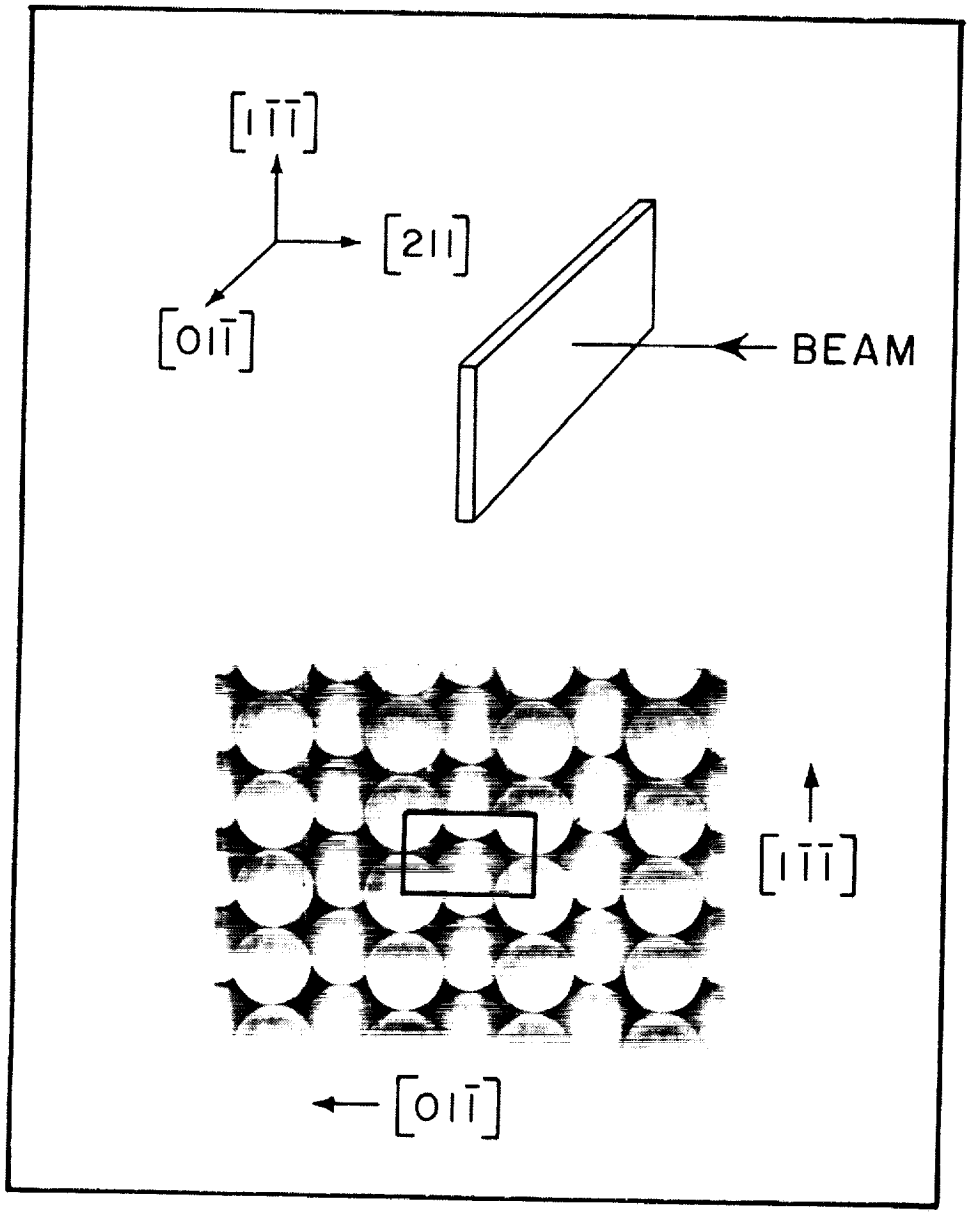

Figure 12

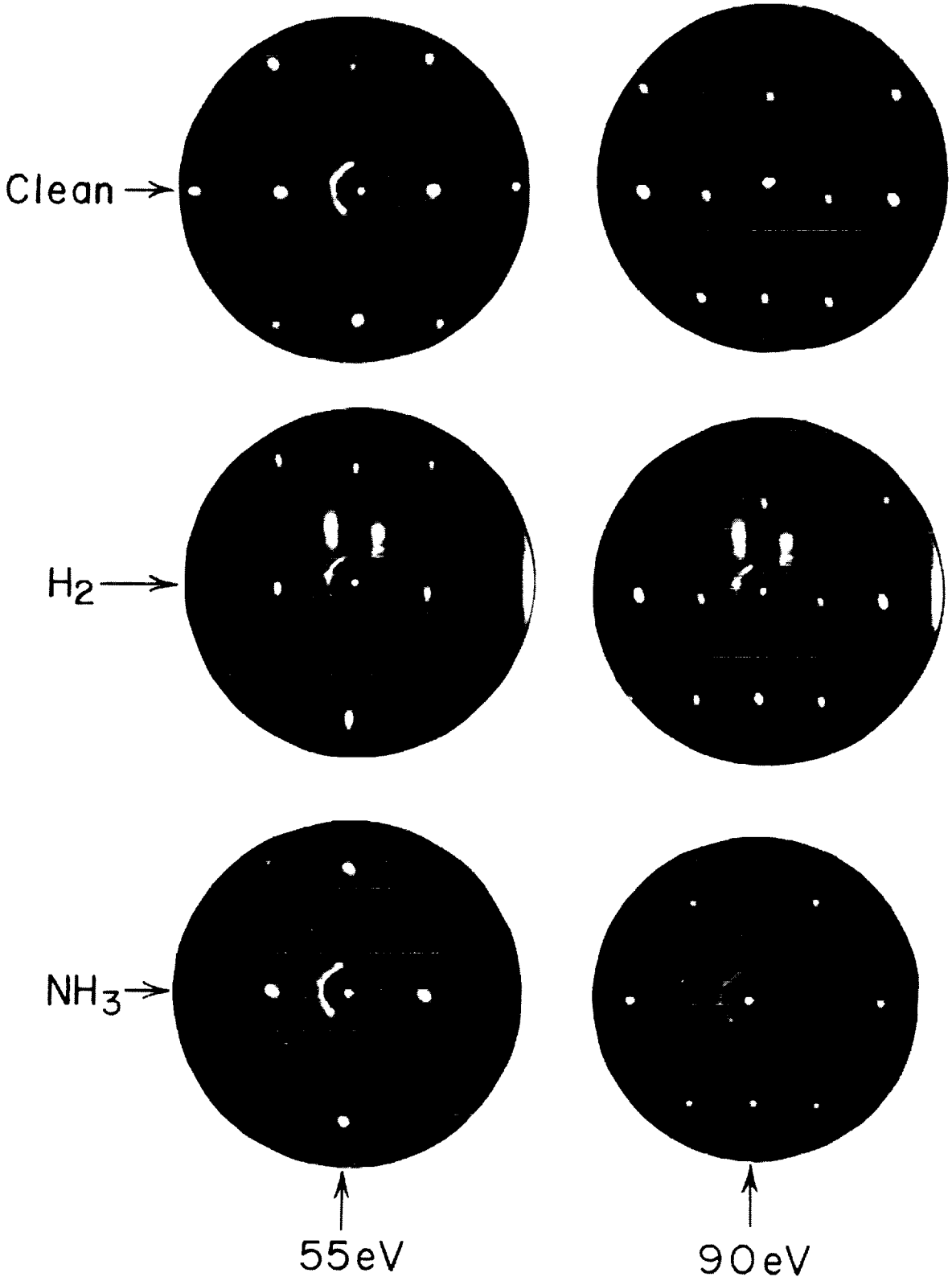

Figure 13

Figure 14

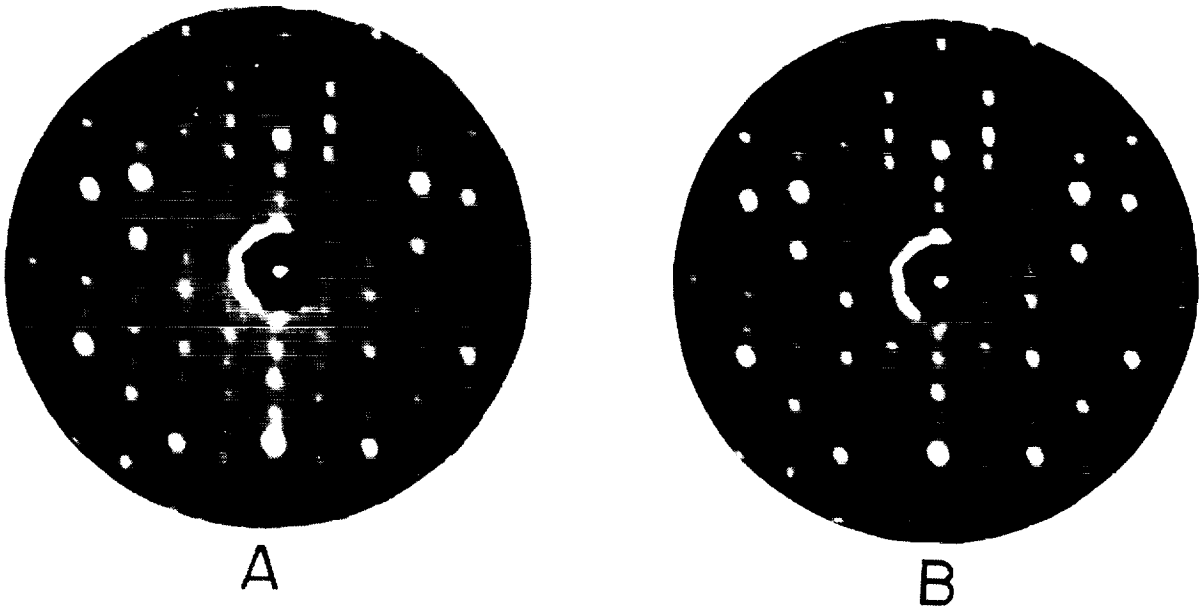

Figure 15

Figure 16

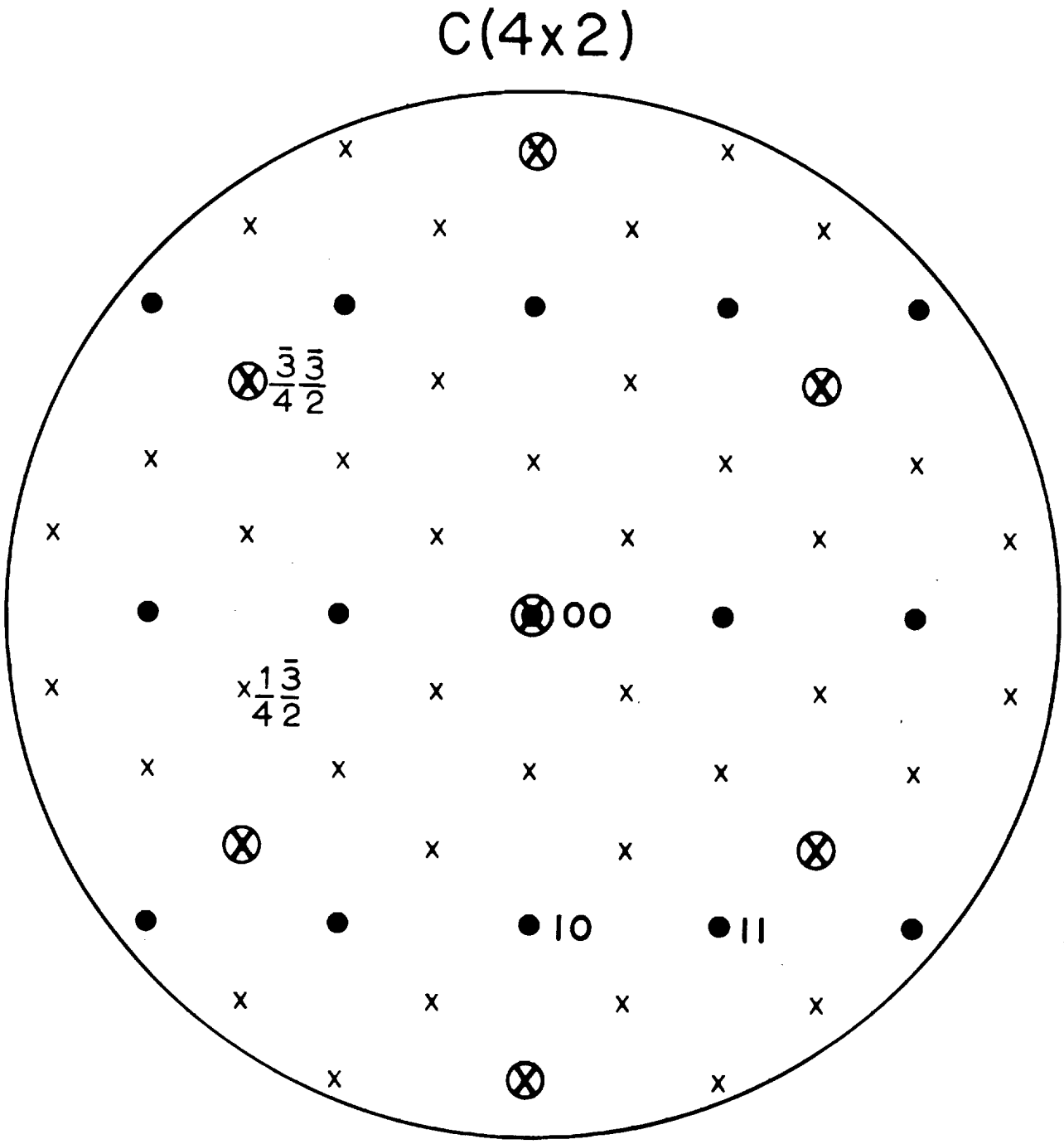
C(4x2)
$\frac{3}{4}\frac{\bar{3}}{2}$
00
$\frac{1}{4}\frac{\bar{3}}{2}$
10
11
● Substrate W(112) Reflections
⊗ Primary Reflections of Overlayer
x Multiple Scattering Beams

Figure 17

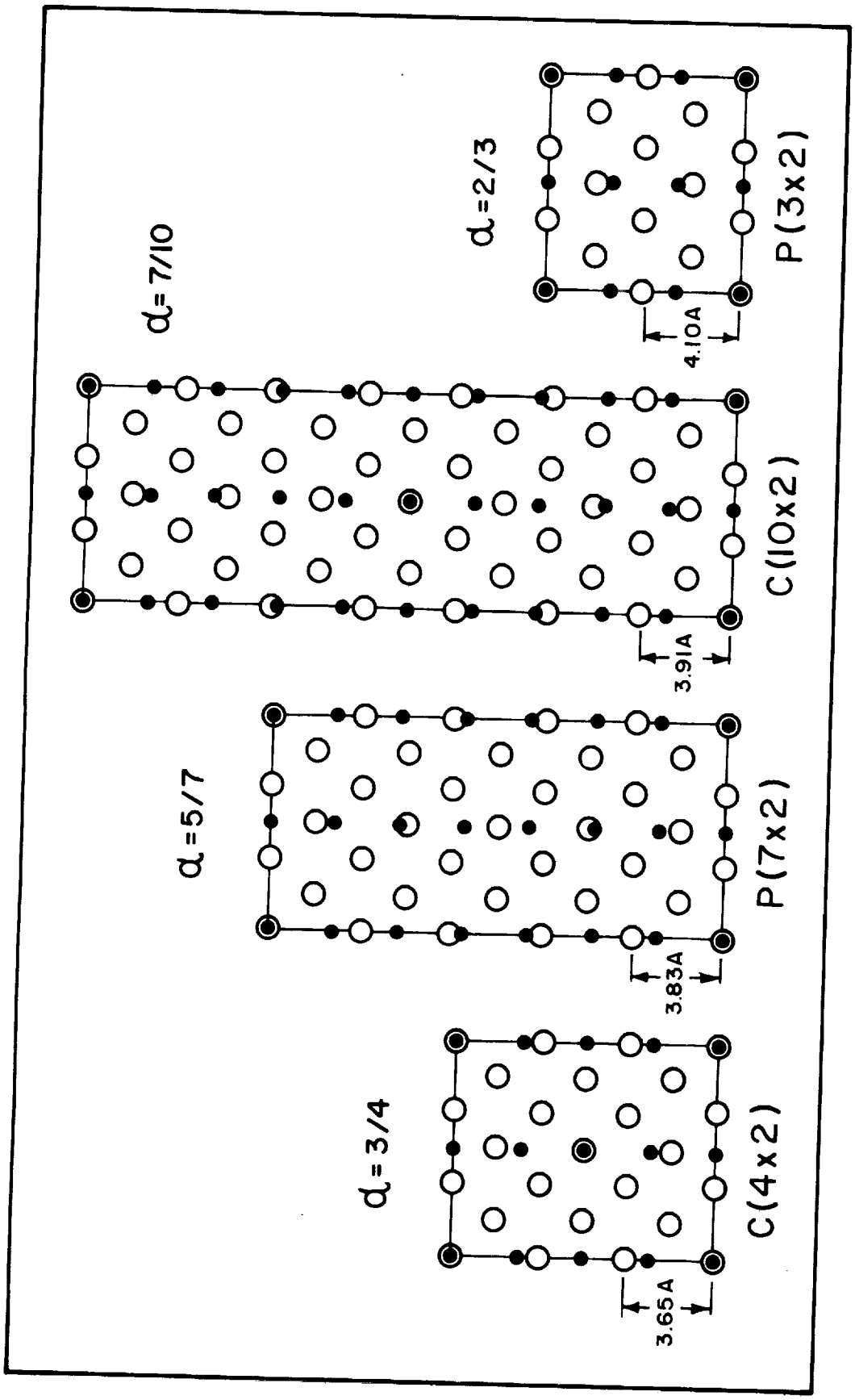

Figure 18

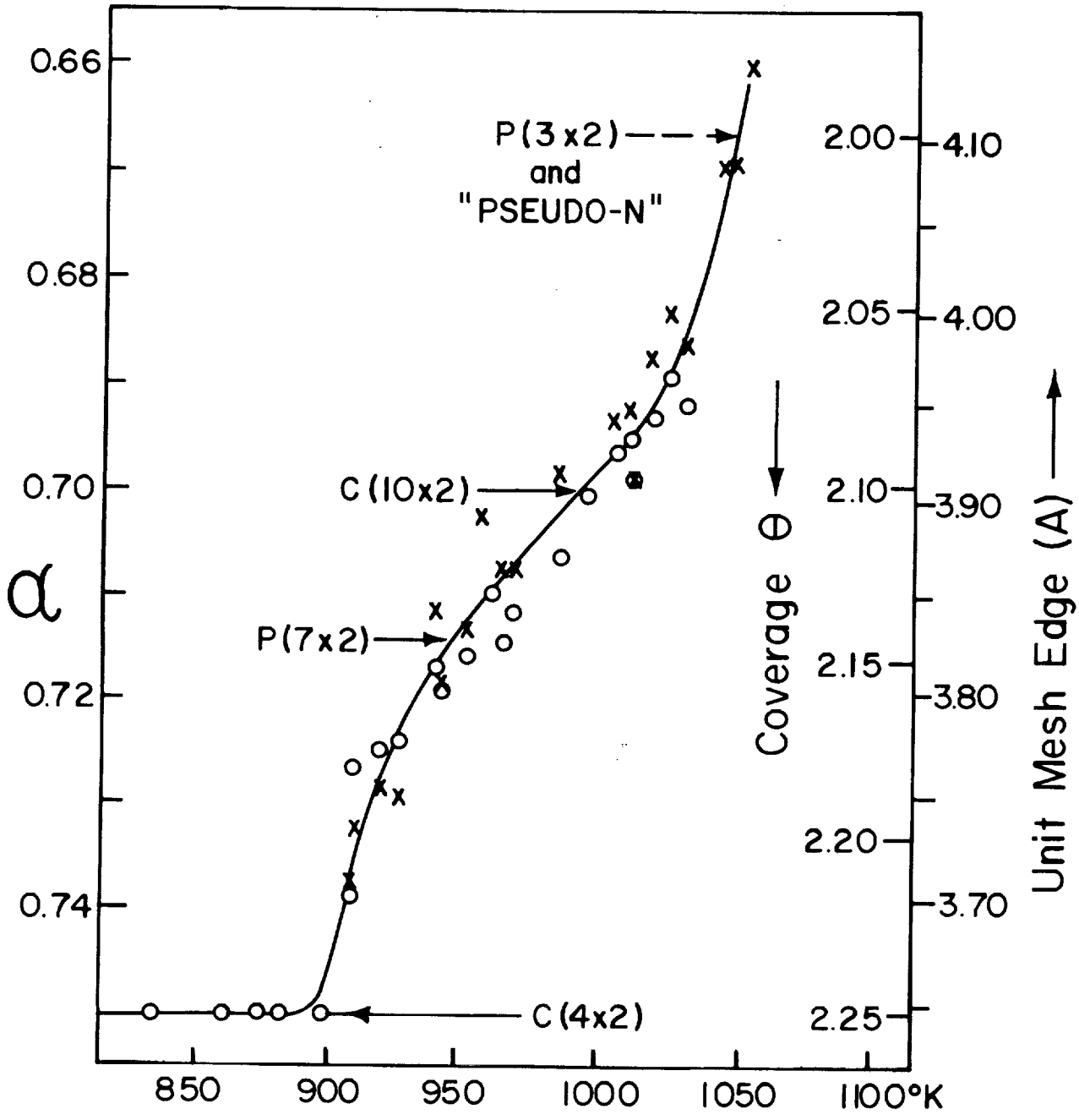
0.66
0.68
0.70
0.72
0.74
α
P(3x2)
and
"PSEUDO-N"
C(10x2)
P(7x2)
C(4x2)
2.00
2.05
2.10
2.15
2.20
2.25
Coverage Θ
4.10
4.00
3.90
3.80
3.70
Unit Mesh Edge (A)
850
900
950
1000
1050
1100°K

Figure 19

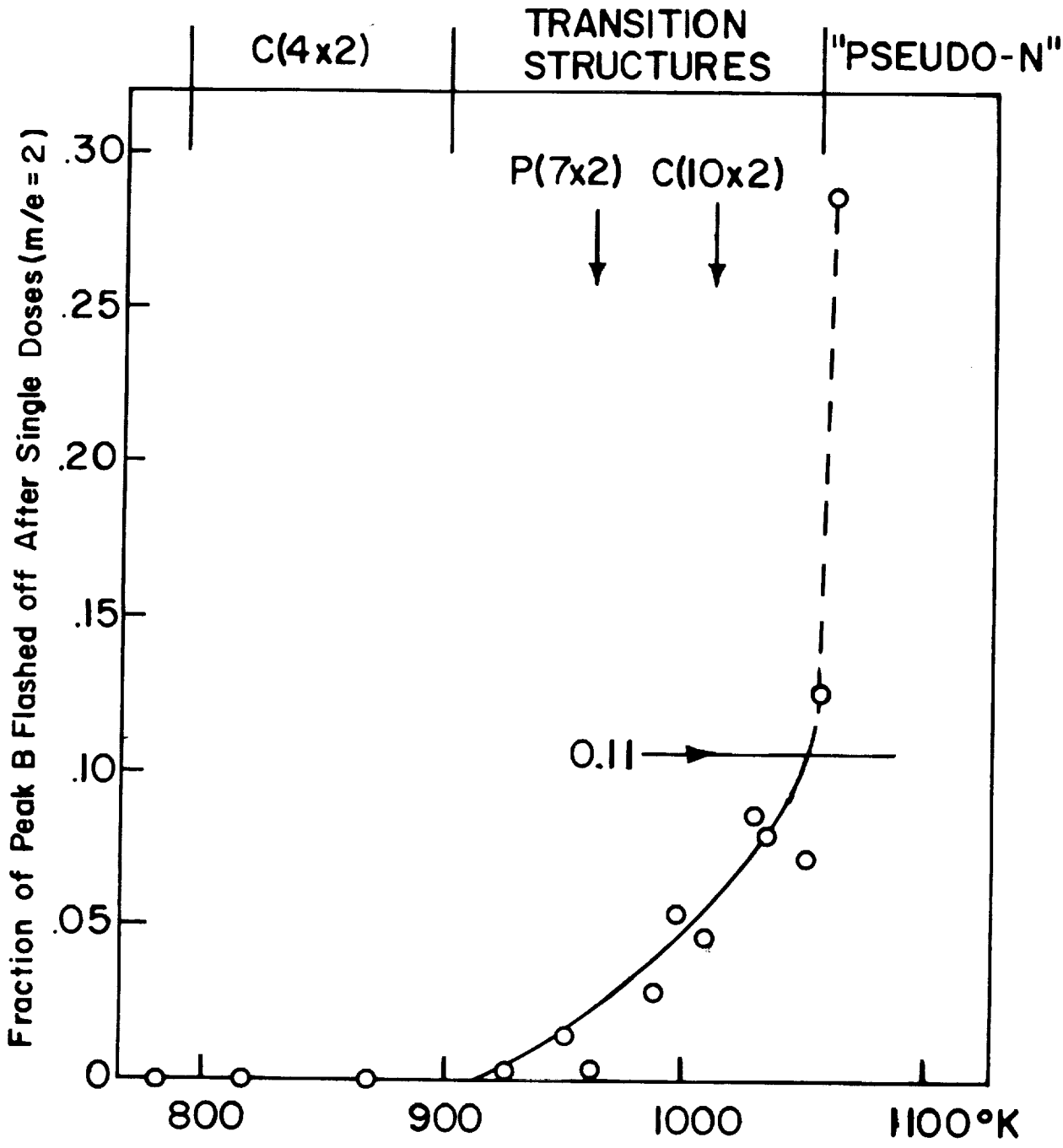
C(4x2)
TRANSITION STRUCTURES
"PSEUDO-N"
P(7x2)
C(10x2)
0.11
Fraction of Peak B Flashed off After Single Doses (m/e = 2)
.30
.25
.20
.15
.10
.05
0
800
900
1000
1100°K

Figure 20

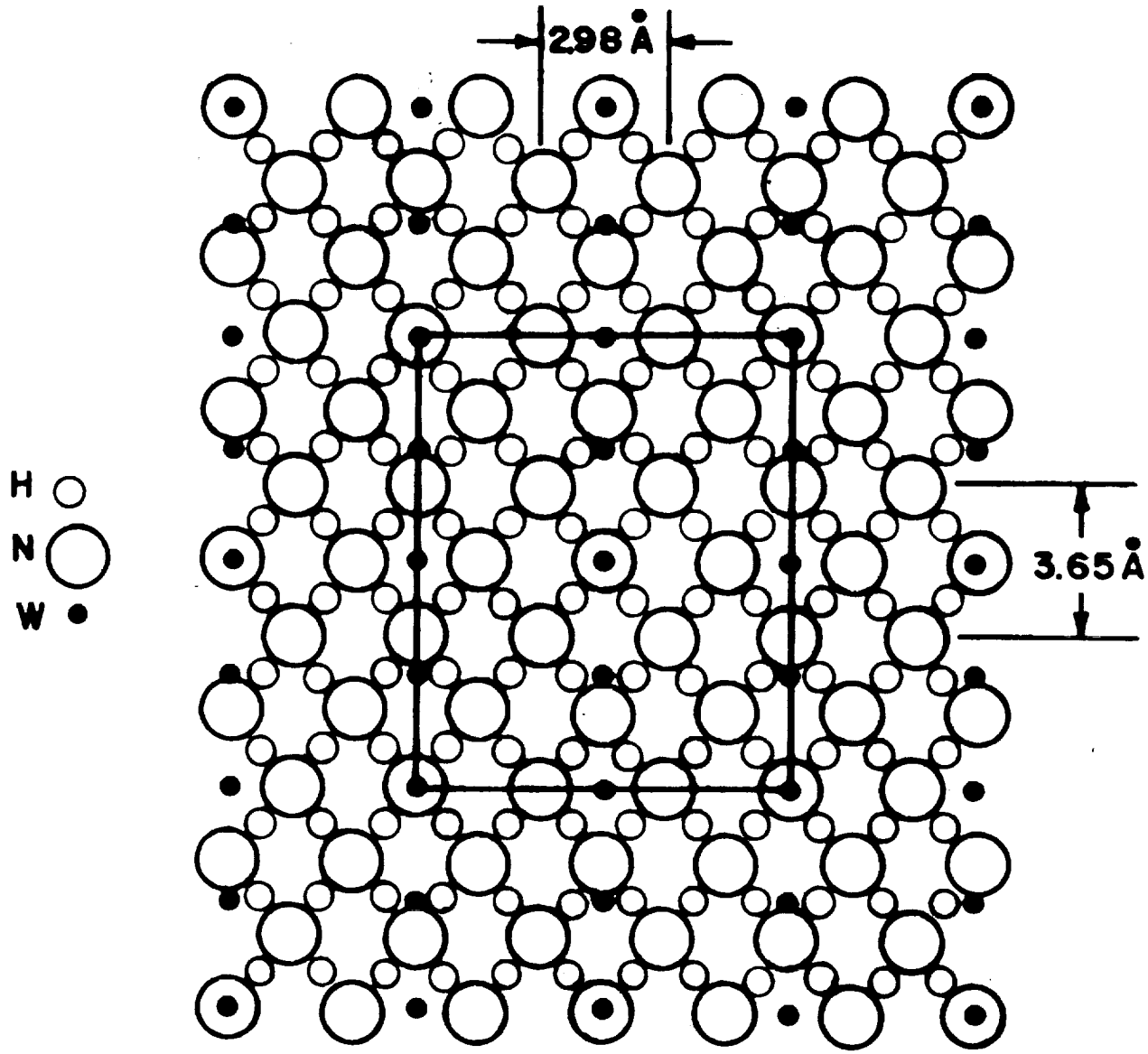

C(4 x 2)

Figure 21

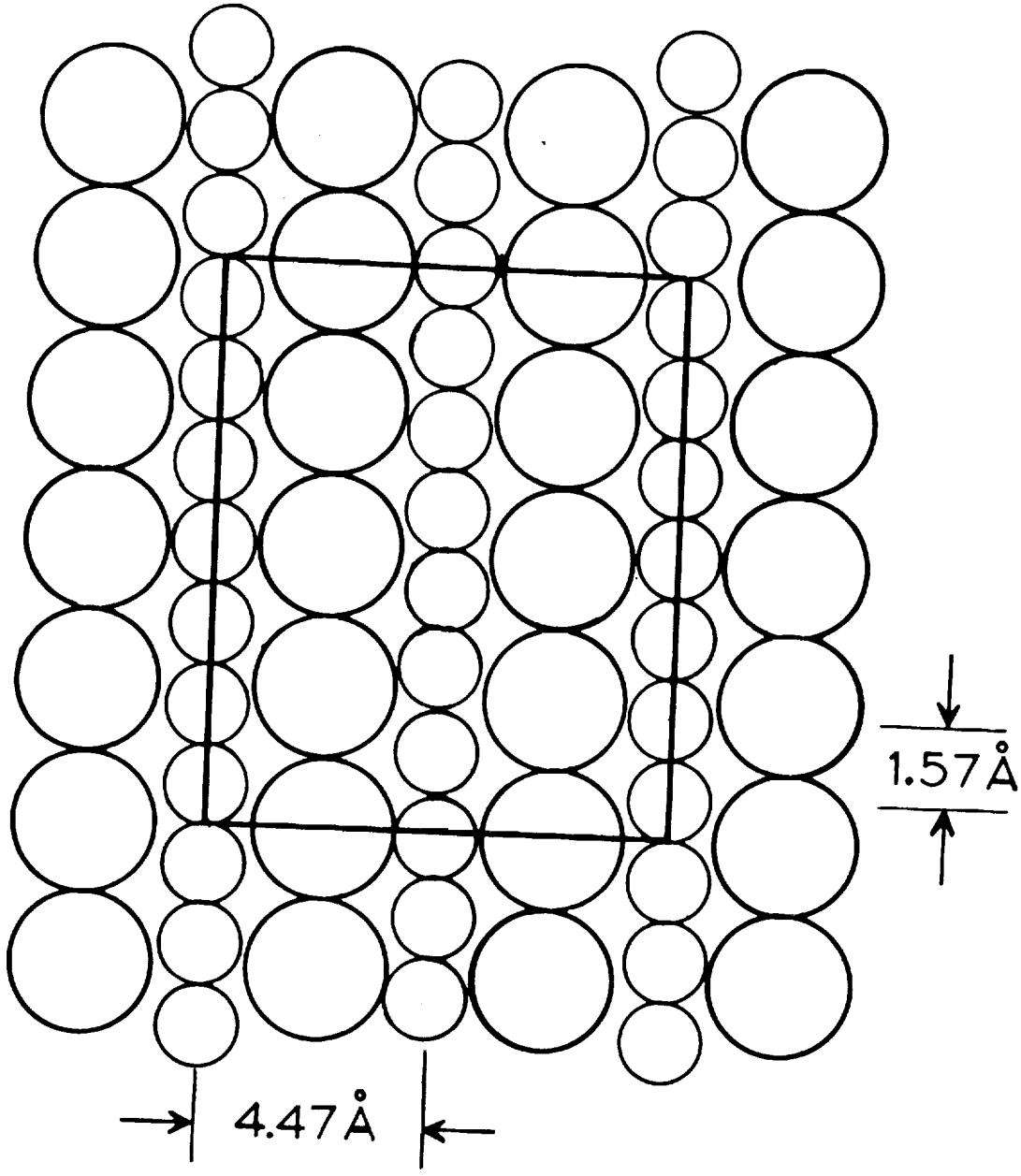

Figure 22

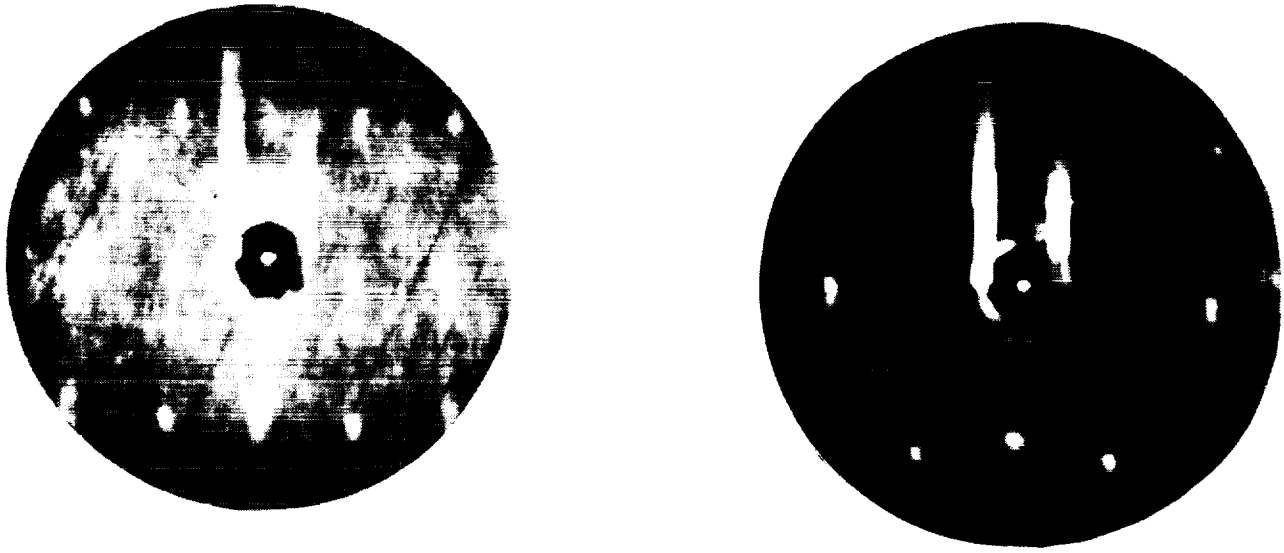

Figure 23

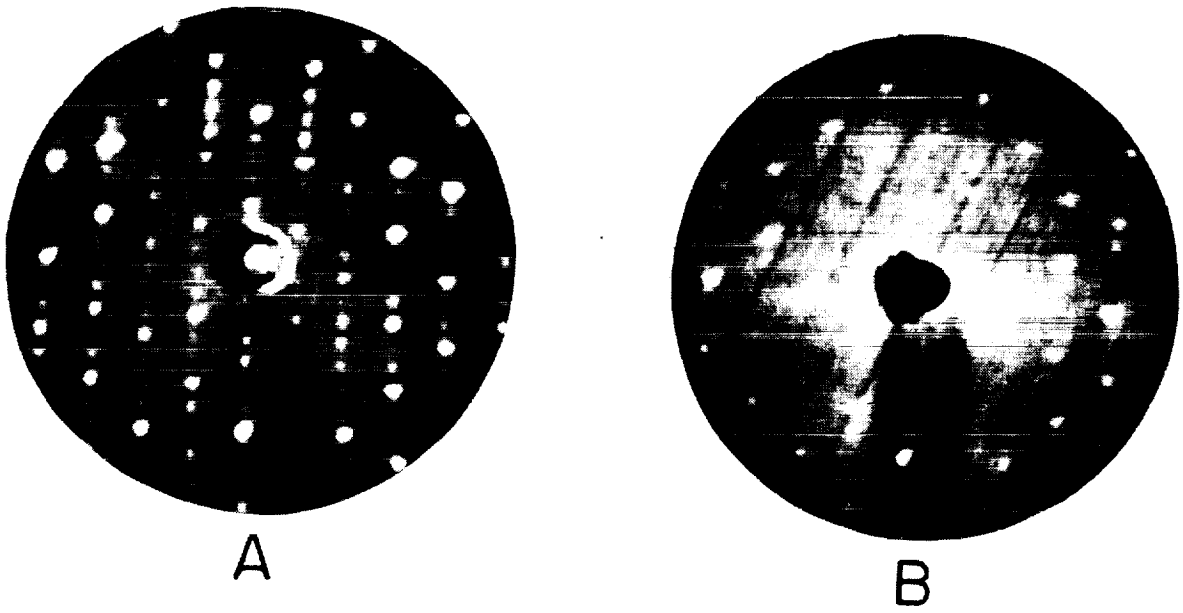

Figure 24

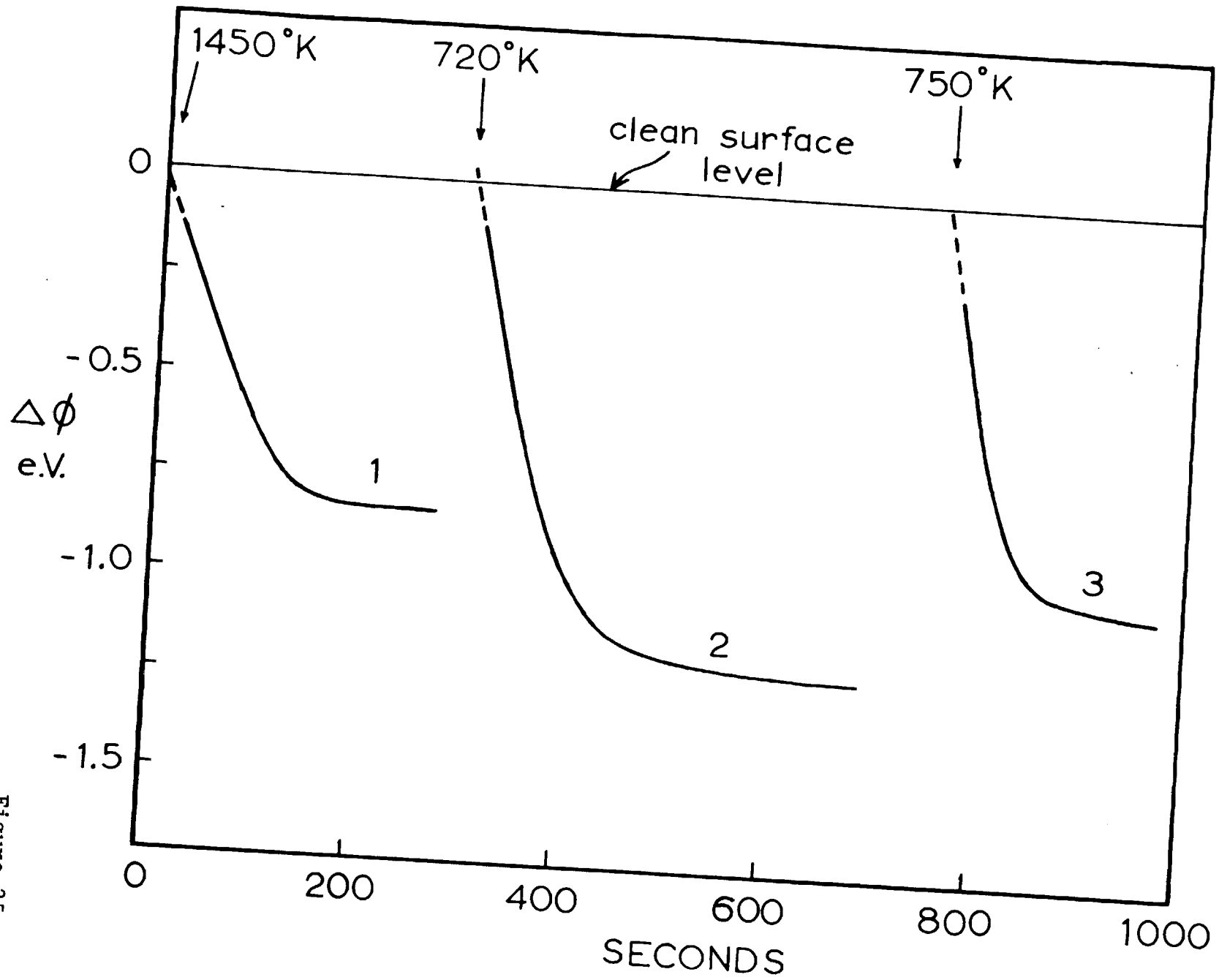
1450°K
720°K
750°K
clean surface level
0
-0.5
-1.0
-1.5
Δφ
e.V.
1
2
3
0
200
400
600
800
1000
SECONDS

Figure 25

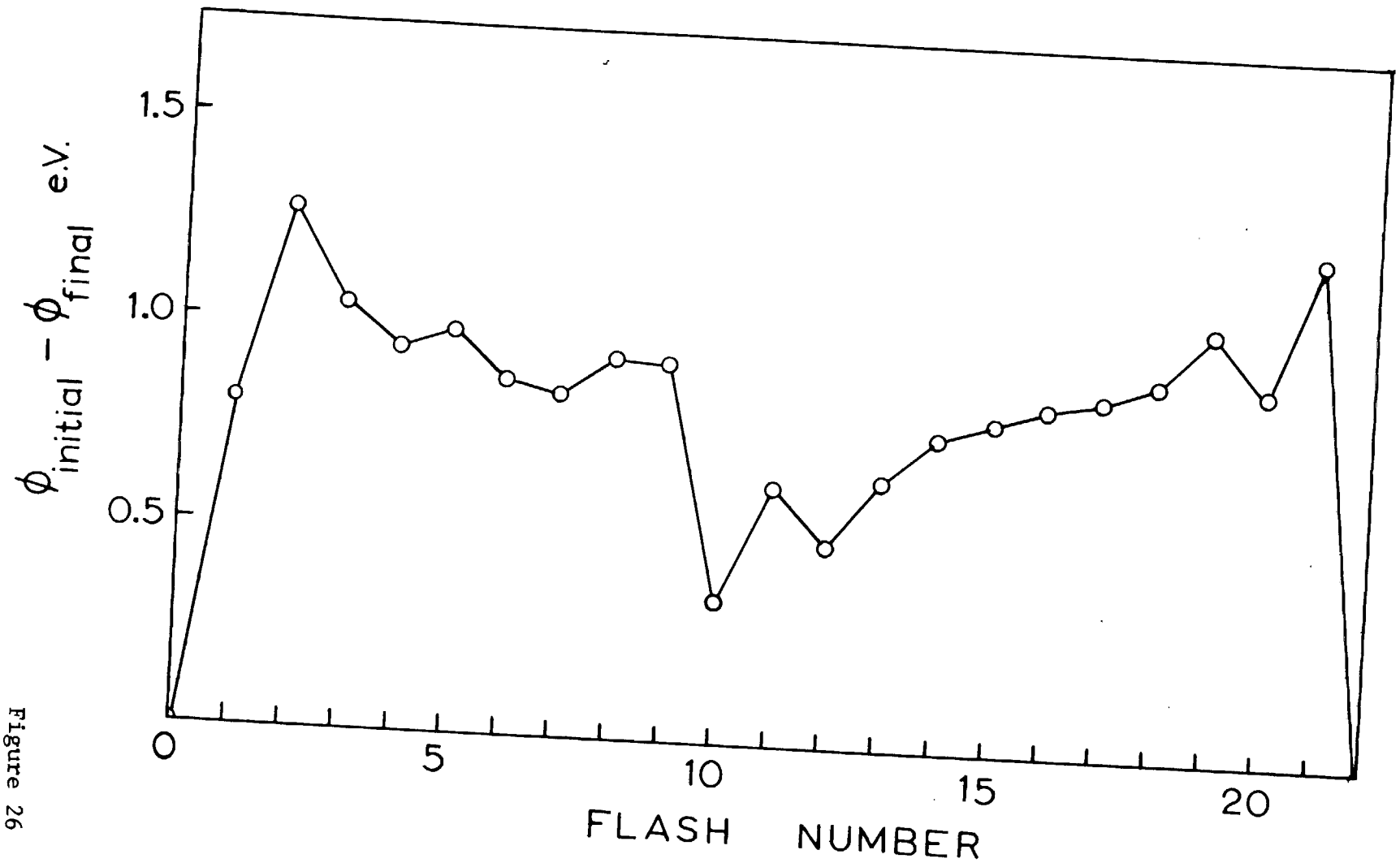

Figure 26

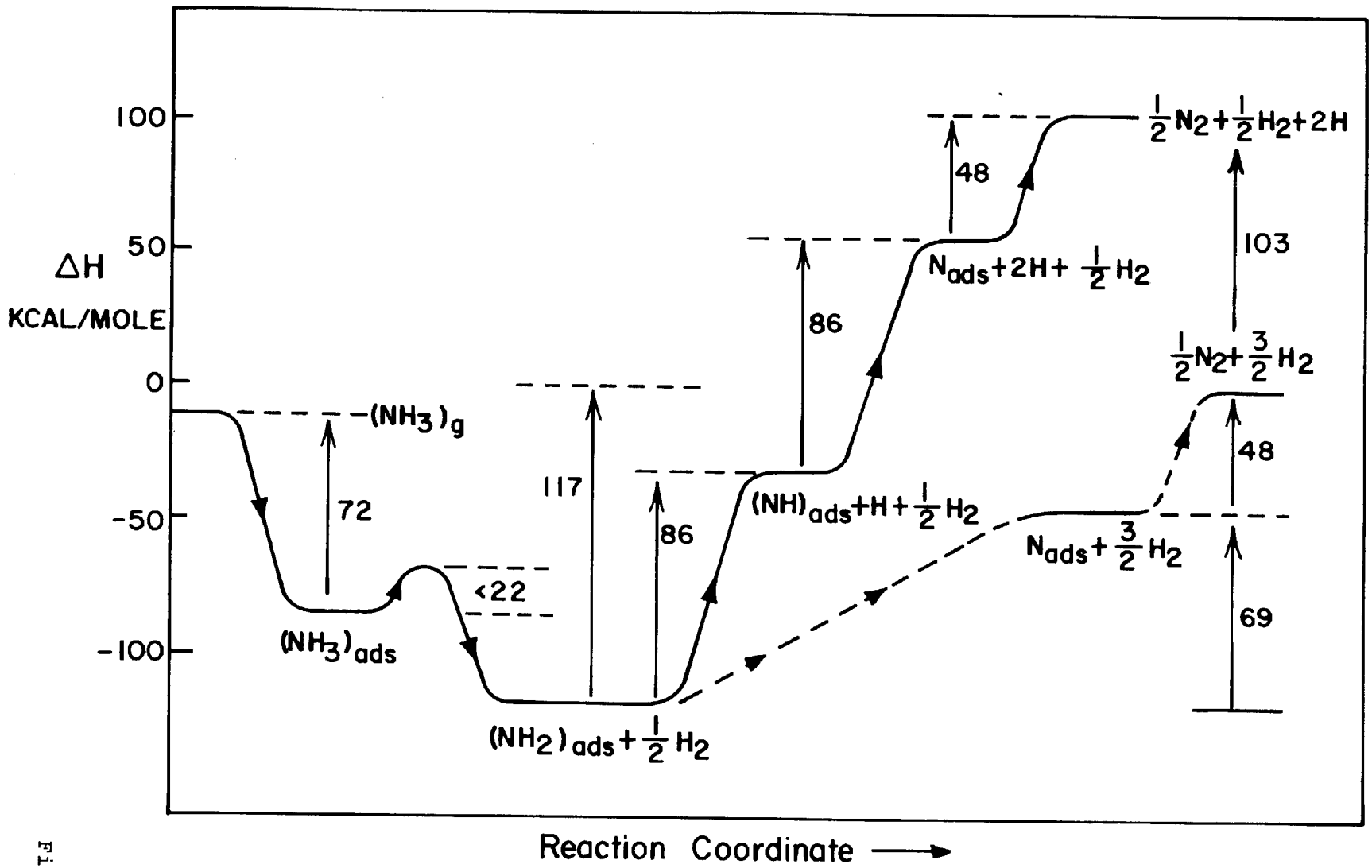
100
50
0
-50
-100
ΔH
KCAL/MOLE
$(NH_3)_g$
72
$(NH_3)_{ads}$
<22
117
86
$(NH_2)_{ads}+\frac{1}{2}H_2$
$(NH)_{ads}+H+\frac{1}{2}H_2$
86
48
$N_{ads}+2H+\frac{1}{2}H_2$
$\frac{1}{2}N_2+\frac{1}{2}H_2+2H$
103
$\frac{1}{2}N_2+\frac{3}{2}H_2$
48
$N_{ads}+\frac{3}{2}H_2$
69
Reaction Coordinate ⟶

Figure 27